

The mystery of the
macho crocs p. 859

Exploring an asthma drug
for Parkinson's pp. 869 & 891

Blue-light photoenzyme builds
hydrocarbons pp. 872 & 903

Science

\$15
1 SEPTEMBER 2017
sciencemag.org

AAAS

LEAF SIZE

Why tropical leaves
are larger p. 917

PLANT ECOLOGY

Global climatic drivers of leaf size

Ian J. Wright,^{1*} Ning Dong,^{1,2} Vincent Maire,^{1,3} I. Colin Prentice,^{1,4} Mark Westoby,¹ Sandra Díaz,⁵ Rachael V. Gallagher,¹ Bonnie F. Jacobs,⁶ Robert Kooyman,¹ Elizabeth A. Law,^{1,7} Michelle R. Leishman,¹ Ülo Niinemets,⁸ Peter B. Reich,^{9,10} Lawren Sack,¹¹ Rafael Villar,¹² Han Wang,^{1,13} Peter Wilf¹⁴

Leaf size varies by over a 100,000-fold among species worldwide. Although 19th-century plant geographers noted that the wet tropics harbor plants with exceptionally large leaves, the latitudinal gradient of leaf size has not been well quantified nor the key climatic drivers convincingly identified. Here, we characterize worldwide patterns in leaf size. Large-leaved species predominate in wet, hot, sunny environments; small-leaved species typify hot, sunny environments only in arid conditions; small leaves are also found in high latitudes and elevations. By modeling the balance of leaf energy inputs and outputs, we show that daytime and nighttime leaf-to-air temperature differences are key to geographic gradients in leaf size. This knowledge can enrich “next-generation” vegetation models in which leaf temperature and water use during photosynthesis play key roles.

Leaf temperature is a key control on plant metabolic rates. Photosynthetic carboxylation increases strongly with temperature, but so too do catabolic processes such as dark respiration and photorespiration (1). Thus, net photosynthetic rate tends to peak at intermediate temperatures, with the optimum temperature typically higher in species from warmer regions (2, 3). Very high or low temperatures can impair enzyme function, disrupt membranes and cellular processes, and if sufficiently extreme, cause irreparable tissue damage (1). Plants show a variety of adaptations for increasing the proportion of the day that leaves can operate in near-optimal temperature ranges

for photosynthesis and for avoiding temperature extremes (4, 5). Pendulous leaves with reflective leaf surfaces may avoid high midday temperatures (6), for example, whereas clumped canopy arrangements in alpine plants help to avoid extreme cold (7). Nonetheless, the most conspicuously varying trait that affects leaf temperature is the size of individual leaves.

Across the plant kingdom, leaves vary from less than 1 mm² to greater than 1 m² in area (8). Larger leaves have a thicker boundary layer that slows sensible heat exchange with the surrounding air, meaning that—all else equal—they develop larger leaf-to-air temperature differences than that of smaller leaves (9, 10). All leaves are cooled by transpirational water loss, but this is particularly critical for large leaves, which face greater risk of potentially serious heat damage at high air temperatures and high irradiance, especially when soil water is limiting (2). These principles are central to well-known theories for optimal leaf size based on daytime leaf energy budgets (2, 9, 11–14), which predict disadvantages to being large-leaved at hotter, drier, and high-irradiance sites. In support of these predictions, many studies have shown smaller mean leaf sizes at sites with lower mean annual precipitation (MAP) (15–19) and higher irradiance (6, 20). However, two recent broad-scale surveys of leaf size versus mean annual temperature (MAT) (18, 19) have shown the opposite pattern to that predicted from these daytime energy budget considerations: mean leaf size clearly increases rather than decreases with MAT (21). These results pose a substantial challenge to accepted understanding based on “classic” energy budget theory. In other studies, large-leaved species have been shown as uncommon at cold, high-elevation sites (7, 22). This pattern instead accords with control by the nighttime energy balance—an under-appreciated influence—which indicates substantial disadvantage for large leaves in cold regions; they are more prone

to frost damage because a thicker boundary layer slows sensible heat exchange with the soil, air, and surrounding vegetation, which is required to offset long-wave radiation losses to the nighttime sky (23, 24).

In this study, our first goal was global-scale quantification of how leaf size varies with site climate, allowing us to analyze the potentially interactive effects of site temperature, irradiance, and moisture and to provide robust tests of predictions from classic optimality-based theories for leaf size (2, 9, 11–14). Our second objective was to model the upper limit to viable leaf sizes in relation to the risks of night-chilling as well as daytime over-heating. By combining analysis of a large worldwide data set with a mechanistic approach to predicting maximum leaf sizes as a function of site climate, we sought to explain the latitudinal gradient in leaf sizes first noted by 19th-century plant geographers (25, 26)—a long-standing ecological conundrum, whose persistence has prevented realistic embedding of this key trait in global vegetation and Earth system models.

We compiled a leaf size data set for 7670 species from 682 nonagricultural sites worldwide, with sampling spread across all vegetated continents, climate zones, biomes, and major growth forms (figs. S1 and S2). At each site, leaf size data were aggregated to a single mean value per species, yielding 13,705 species-site combinations. “Leaf size” here refers to the one-sided projected area of single leaves, leaflets (for compound-leaved species), or leaf analogs (such as phyllodes and cladodes) for otherwise leafless species. Annual and growing-season climate data for each site were derived from source publications or from global climate data sets. Leaf size varied among species by more than five orders of magnitude. On average, trees had larger leaves than shrubs, herbs, or grasses (fig. S2), but very substantial variation could be observed within each growth form. There was also strong taxonomic patterning; for example, families such as Dipterocarpaceae and Magnoliaceae were characterized by many large-leaved species, whereas many small-leaved species were found in Cupressaceae, Ericaceae, and Fabaceae.

Leaf size was on average larger in equatorial regions and smaller toward the poles. A quadratic regression fit to latitude explained 28% of global variation (Fig. 1A), with near-identical trends in simple-leaved and compound-leaved species (fig. S3). Similar or even higher explanatory power was observed within major clades (fig. S4). Common climate metrics associated with latitude explained smaller but still substantial proportions of leaf size variation (Fig. 1 and table S2): MAP (Fig. 1B) and MAT explained 22 and 15% of the global variation, respectively (larger leaves at wetter or warmer sites). Other variables related to site moisture explained less variation than did MAP [such as moisture index (MI), the ratio of annual precipitation to potential evapotranspiration, coefficient of determination (R^2) = 0.12 (Fig. 1C)]. For site temperature, the strongest relationships to leaf size, all positive in sign, were

¹Department of Biological Sciences, Macquarie University, NSW 2109, Australia. ²Centre for Past Climate Change and School of Archaeology, Geography and Environmental Sciences (SAGES), University of Reading, Whiteknights, RG6 6AH Reading, UK. ³Université du Québec à Trois-Rivières, Trois-Rivières, QC G9A 5H7, Canada. ⁴AXA Chair in Biosphere and Climate Impacts, Department of Life Sciences, Imperial College London, Silwood Park Campus, Buckhurst Road, Ascot SL5 7PY, UK. ⁵Instituto Multidisciplinario de Biología Vegetal (IMBIV), Consejo Nacional de Investigaciones Científicas y Técnicas and Facultad de Ciencias Exactas, Físicas y Naturales, Universidad Nacional de Córdoba, Casilla de Correo 495, 5000 Córdoba, Argentina. ⁶Roy M. Huffington Department of Earth Sciences, Southern Methodist University, Dallas, TX 75275, USA. ⁷School of Biological Sciences, University of Queensland, St Lucia, QLD 4072, Australia. ⁸Institute of Agricultural and Environmental Sciences, Estonian University of Life Sciences, Kreutzwaldi 1, Tartu 51014, Estonia. ⁹Department of Forest Resources, University of Minnesota, St. Paul, MN 55108, USA. ¹⁰Hawkesbury Institute for the Environment, Western Sydney University, Penrith 2751, NSW, Australia. ¹¹Department of Ecology and Evolutionary Biology, University of California, Los Angeles, CA 90095, USA. ¹²Área de Ecología, Facultad de Ciencias, Universidad de Córdoba, 14071 Córdoba, Spain. ¹³State Key Laboratory of Soil Erosion and Dryland Farming on the Loess Plateau, College of Forestry, Northwest A & F University, Yangling 712100, China. ¹⁴Department of Geosciences, Pennsylvania State University, University Park, PA 16802, USA.

*Corresponding author. Email: ian.wright@mq.edu.au

with climate variables expressed on a growing season basis [mean growing season temperature, $R^2 = 0.21$ (Fig. 1D); mean temperature of the coldest month during the growing season, $R^2 = 0.24$]. Leaf size was statistically correlated with irradiance, but with little explanatory power ($R^2 < 0.01$, $P = 0.002$) (Fig. 1E). In general, relationships between leaf size and individual climate variables were tighter in woody than in nonwoody species and, among woody taxa, tighter in evergreen than in deciduous species (tables S3 and S4).

Combinations of climate variables explained the most variation in leaf size. Site temperature [most notably, mean temperature during the warmest month (T_{WM})], irradiance, and moisture (MAP or MI) showed strong interactive effects, with best-fit surfaces being twisted planes (Fig. 2 and fig. S5). At the driest sites (MAP < ~800 mm or MI < ~0.5), leaf size weakly decreased with T_{WM} , whereas across wetter sites, leaf size increased with T_{WM} ($R^2 = 0.34$) (Fig. 2). This coupling with site temperature was increasingly steep and tight at higher MAP (fig. S6A). Similarly, leaf size was unrelated to MAP at colder sites (T_{WM} in the range from 0° to 15°C) but was positively related to MAP at warmer sites, and increasingly so the higher the T_{WM} (fig. S6C). Qualitatively similar patterns with similar explanatory power were found when substituting irradiance for T_{WM} in these analyses (figs. S5 and S6, B and D), or MI for MAP ($R^2 = 0.33$): Leaves were smaller at drier sites only in warm regions, smaller at hotter or higher irradiance sites only in dry regions, and smaller at colder sites, especially under wetter conditions. That is, each of the individual predictions from previous leaf energy balance theory was supported under specific conditions, but none was universally true.

Our empirical analyses indicated that the upper limits to leaf size showed marked trends both with latitude (quantile regression slopes in Fig. 1A and fig. S4) and climate (fig. S6, A to D; quantile regressions in Fig. 1, B to D, and fig. S5; and table S2). To explore this upper-limit issue more deeply, we developed a simple but robust approach to energy-balance modeling for both daytime and nighttime leaf-to-air temperature differences (fig. S8). Energy balance theory (2, 4) predicts that the net radiation at the leaf surface in steady state must be equal to the sum of sensible and latent heat exchanges with the surrounding air, the former being proportional to the leaf-to-air temperature difference (ΔT), the latter to the transpiration rate. On the basis of this theory, we applied a generic calculation to predict upper bounds on leaf size during the daytime, for each study site. We assumed that plants cannot transpire faster than at the maximum rate allowed by the net radiation balance of the leaf and the temperature of the air, and that the transpiration rate is progressively reduced as soil moisture availability declines. Using the well-established relationship between leaf boundary-layer conductance (g_b) and size (4, 9), we can then derive for any given set of climatic conditions the maximum leaf size that keeps leaf temper-

ature below a specified upper limit throughout the year.

We also considered the energy balance of leaves during the nighttime, when net radiation is negative and the extent to which this is compen-

sated by sensible heat exchange determines ΔT (23, 24). For this calculation of maximum expected leaf size, we specified a lower temperature limit below which active leaves would be expected to suffer serious damage. We considered

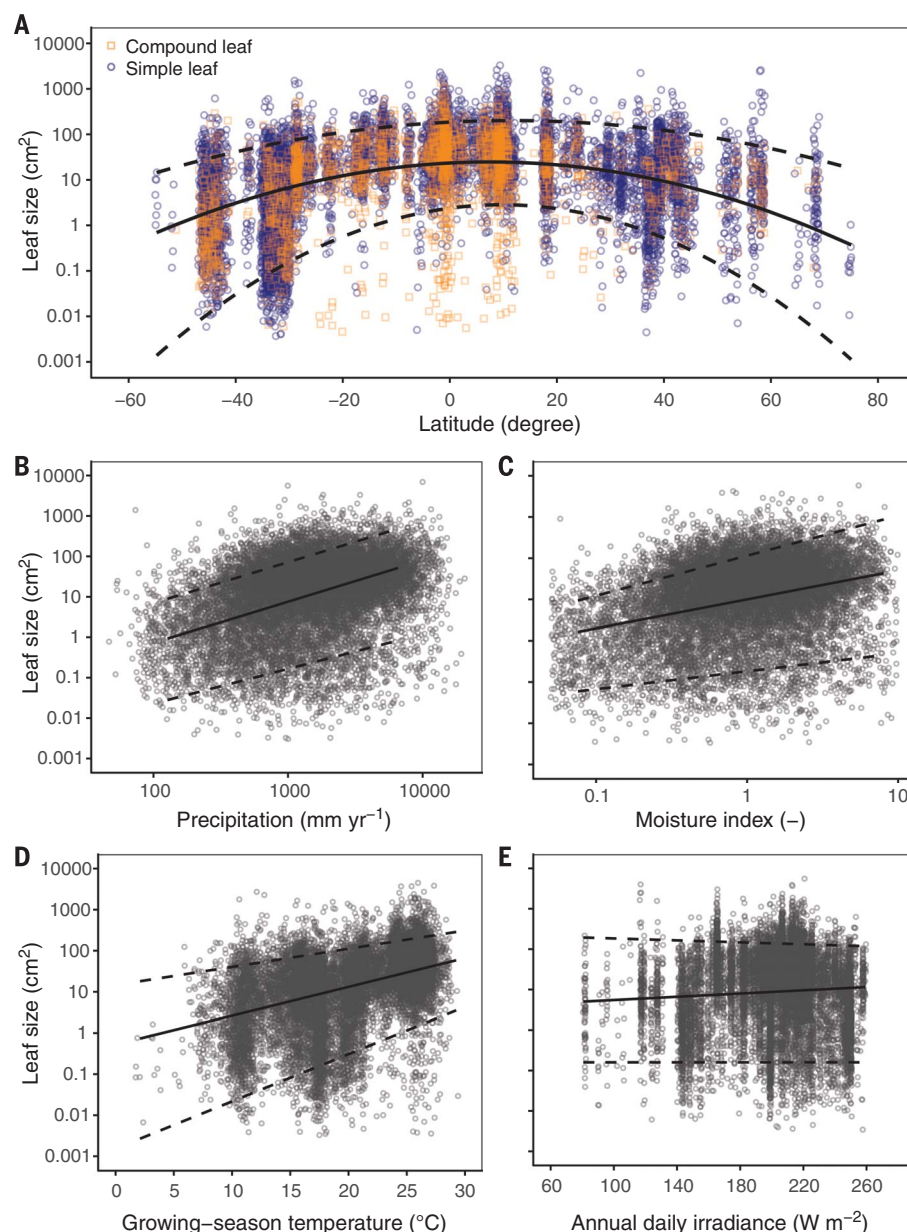


Fig. 1. Global trends in leaf size (LS) in relation to latitude and climate. (A) Species are coded as simple-leaved (blue circles) or compound-leaved (orange squares; for which “leaf size” refers to that of the leaflets). Solid fitted line (quadratic regression, all species), $\log LS = 1.37 + 0.006 \text{ Lat} - 0.0004 \text{ Lat}^2$; $R^2 = 0.28$, $P < 0.0001$. Shown in fig. S3, A and B, are equivalent graphs, with slopes fitted separately to simple- and compound-leaved species, and when considering leaf size of compound leaves to be that of the entire leaf rather than that of the leaflets. (B) Mean annual precipitation ($\log LS = 1.02 \log MAP - 2.18$; $R^2 = 0.22$, $P < 0.0001$). (C) Annual equilibrium MI ($\log LS = 0.70 \log MI + 1.00$; $R^2 = 0.12$, $P < 0.0001$). (D) Mean temperature during the growing season ($\log LS = 0.07 T_{gs} - 0.28$; $R^2 = 0.21$, $P < 0.0001$). (E) Annual daily radiation ($\log LS = 0.002 \text{ RAD} + 0.54$; $R^2 = 0.002$, $P = 0.002$). In (A) to (E), fitted slopes were estimated by using linear mixed models (site and species treated as random effects); further details of leaf size–climate relationships are given in table S2. In (A) to (E), sample $n = 13,641$ species–site combinations and dashed lines show the 5th and 95th quantile regression fits. Further analysis by using quantile regression is presented in fig. S7.

only temperatures encountered during the thermal growing season, on the basis that leaves in the coldest part of the year in cold-winter climates will be shed or cold-hardened and dor-

mant. On the basis of these two constraints—applying an upper leaf temperature limit of 50°C (27, 28), and a lower temperature limit of -5°C (29)—we derived two predictions of maximum

viable leaf size for each of the 682 sites in our data set. From these data, we derived general predictions for latitudinal trends in maximum leaf size and compared them with observed data (Fig. 3 and figs. S9 to S12).

At arid sites ($MI < 0.5$) (Fig. 3A), the upper boundary of leaf size is almost universally consistent with estimated daytime constraints (Fig. 3, red dashed line) because rapid transpiration is impossible when water supply is limited, and large leaves are disadvantaged by reaching damagingly high temperatures. At intermediate-MI sites (Fig. 3B), daytime constraints appear more limiting between ~20° S and 20° N, but nighttime constraints dominate outside this zone. At wet sites ($MI > 1.5$) (Fig. 3C), daytime constraints are predicted to be unimportant because sufficient water is generally available for effective transpirational cooling, with nighttime constraints dominating at all latitudes.

These results can be generalized in the form of global maps showing geographic trends in maximum leaf size (Fig. 4) and its determinants (fig. S13). Maximum viable leaf sizes are shown to be especially small both in warm deserts and cold, high-elevation regions (such as Tibet and the Andes), but for different reasons relating to daytime and nighttime constraints, respectively. Steep gradients of predicted maximum leaf size can be found, for example, where arid subtropics transition into wet tropics. In very warm (day and night), ever-wet climates, there may be no effective thermal constraint on leaf size (figs. S4, deep blue shade, and S13, “unlimited” category). In these situations, it is likely that other limits to leaf size come into play, such as the biomechanics of support (6) or whole-plant hydraulic architecture (30). We estimate that these situations represent 4.3%

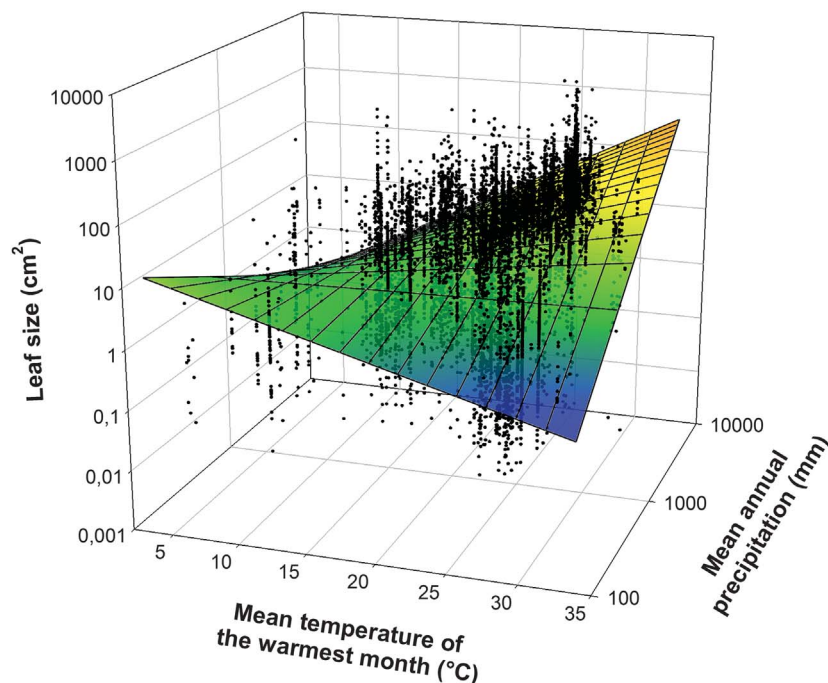


Fig. 2. Global variation in leaf size as a function of site temperature and precipitation. Considering leaf size (LS) as a function of mean temperature of the warmest month (T_{WM}) and mean annual precipitation (MAP), the best-fit surface estimated by multiple mixed-model regression was a twisted plane with the form $\log LS = -0.27 T_{WM} - 1.32 \log MAP + 0.10 T_{WM} \times \log MAP + 4.01$ (all parameters $P = 0.001$; $R^2 = 0.34$; $n = 13,641$ species-site combinations). Similar results were found in analyses involving irradiance rather than T_{WM} , or annual moisture index (MI) rather than precipitation (figs. S5 and S6).

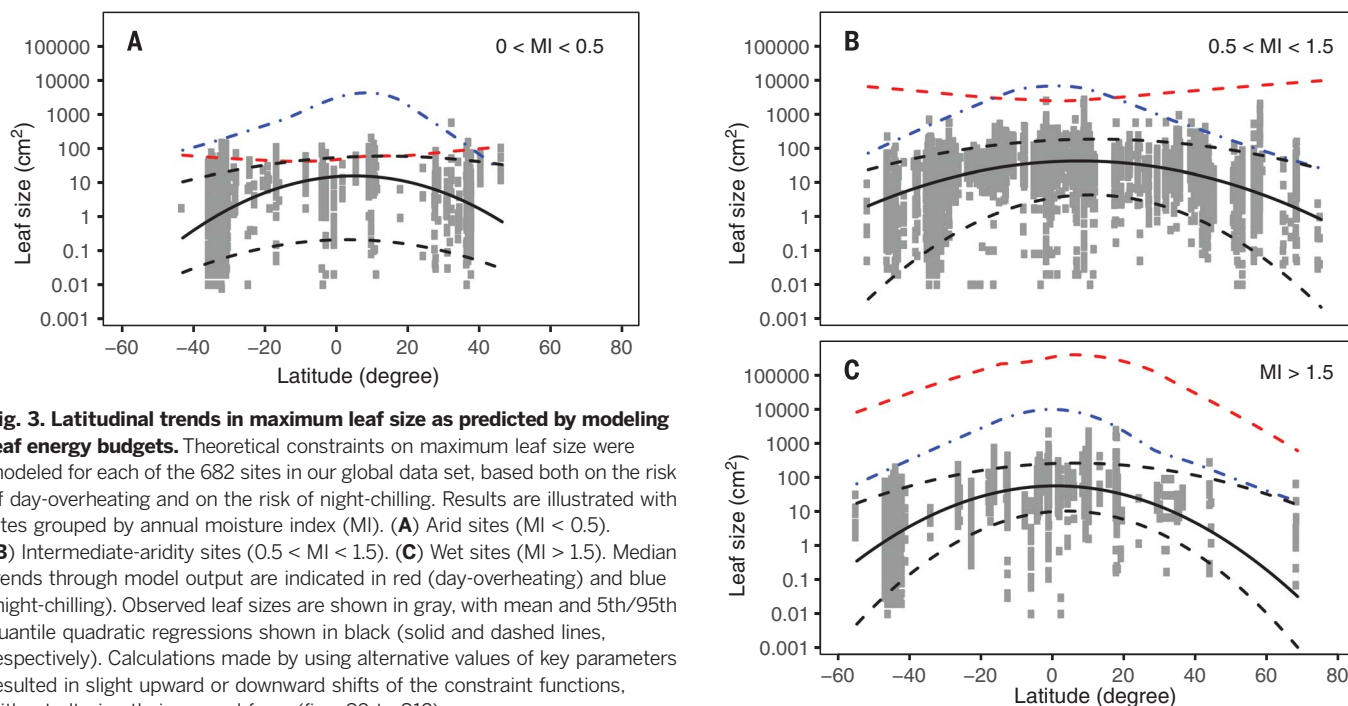


Fig. 3. Latitudinal trends in maximum leaf size as predicted by modeling leaf energy budgets. Theoretical constraints on maximum leaf size were modeled for each of the 682 sites in our global data set, based both on the risk of day-overheating and on the risk of night-chilling. Results are illustrated with sites grouped by annual moisture index (MI). (A) Arid sites ($MI < 0.5$). (B) Intermediate-aridity sites ($0.5 < MI < 1.5$). (C) Wet sites ($MI > 1.5$). Median trends through model output are indicated in red (day-overheating) and blue (night-chilling). Observed leaf sizes are shown in gray, with mean and 5th/95th quantile quadratic regressions shown in black (solid and dashed lines, respectively). Calculations made by using alternative values of key parameters resulted in slight upward or downward shifts of the constraint functions, without altering their general form (figs. S9 to S12).

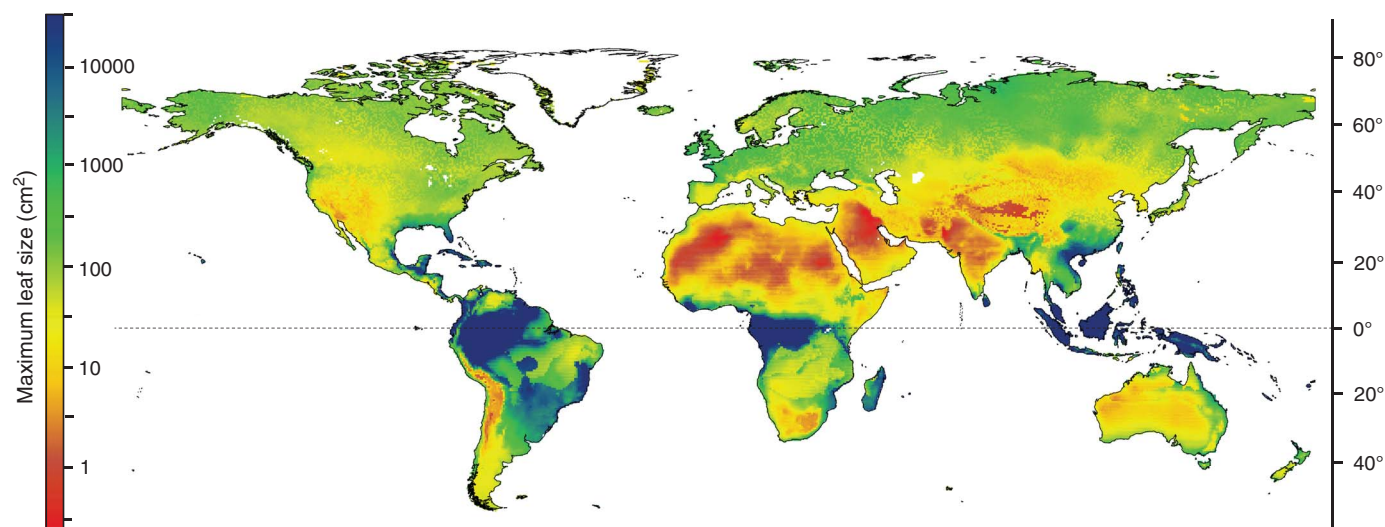


Fig. 4. Predicted geographic trends in maximum leaf size. Each grid cell is color coded according to the smaller of the two predictions for maximum leaf size (daytime or nighttime) (fig. S13), made by using the same procedure as the site-specific modeling. Areas coded the deepest shade of

blue are those where there may be no effective thermal constraint on maximum leaf size because sufficient water is generally available for effective transpirational cooling, and warm nighttime air temperatures prevent leaves from suffering radiative frost damage.

of global land area, whereas nighttime constraints provide the dominant control for 51%, daytime constraints 38%, and night and day constraints colimit leaf sizes for 6.7% of land (fig. S13).

Our model is based on a first-order empirical approximation to transpiration that can be derived in terms of boundary-layer theory (31, 32). It is likely to be more accurate for canopy species. All else being equal, lower energy inputs in shaded situations may allow for larger leaf sizes than predicted (6, 11–13, 33), whereas shallow-rooted species with restricted access to water might have smaller leaf sizes than predicted (34). More explicit modeling of leaf-level energy balance is possible. However, consideration of, for example, vertical gradients of leaf size would also entail modeling of within-canopy humidity and wind speeds, which is a more complex task.

What are the selective advantages that favor large leaves under conditions when they are physiologically possible? This is not well understood, but two prospective explanations seem most promising. First, by deploying a given leaf mass as fewer, larger leaves, the associated twig costs tend to be lower (13, 35), even if within-leaf structural costs are higher (36). All else being equal, this should lead to a growth advantage (37). Second, the wider leaf-to-air temperature differences possible for larger leaves may allow them to more quickly heat up to favorable temperatures for photosynthesis during cool mornings, leading to substantially higher photosynthetic returns (5). In addition, under sufficiently hot and high-irradiance conditions, wider leaf-to-air temperature differences may allow larger leaves to operate at temperatures substantially lower than that of the surrounding air (and more favorable for photosynthesis), provided sufficient soil water is available to support the necessary transpiration (9, 38, 39).

A wide range of leaf sizes exists at any given climate or latitude (Fig. 1). Leaf size is coordinated with many other features of plant architecture, canopy display, and plant hydraulics (6, 7, 13, 30, 35, 40), apparently leading to many equally viable leaf size strategies for a given climate. Additional factors are known to influence leaf size; most notably, low-nutrient soils are characterized by smaller-leaved species (6, 17), smaller-leaved species seemingly suffer less herbivory (41), and as already noted, larger leaves may be favored under deep shade (6, 11–13, 33). Nonetheless, it appears that climate provides the dominant control on the global geographic limits to leaf size, acting both through daytime and nighttime constraints. The nighttime constraint on leaf size in seasonally cold climates has featured in literature on alpine regions and on frost risks in agriculture (23, 24), but its generality has not previously been noted.

Our analyses have moved beyond consideration of bivariate leaf size–climate relationships (6, 7, 15–22), and in doing so, they show simple, interpretable patterns that had not emerged from previous analyses of more limited sets of observations. By pairing broad-scale data synthesis with a simple and robust approach to leaf energy balance modeling, we have shown that the key to understanding geographical limits to leaf size is the leaf-to-air temperature difference, which reflects the balance of energy inputs and outputs. This approach provides a quantitative explanation for the latitudinal gradient in leaf size, one of the oldest observations in ecology (25, 26), for which no general theory existed previously. This knowledge has the potential to enrich “next-generation” vegetation models, in which leaf temperature and water use during photosynthesis play key roles, and to constrain predictions from species distribution models in relation to climate

change. It will aid reconstruction of paleoclimate from leaf macrofossils (15, 16, 19, 21), an enterprise that also dates back more than a century (42) but which, until now, has relied entirely on empirical relationships between leaf traits and climate.

REFERENCES AND NOTES

1. H. G. Jones, *Plants and Microclimate: A Quantitative Approach to Environmental Plant Physiology* (Cambridge Univ. Press, ed. 3, 2014).
2. D. M. Gates, *Ecology* **46**, 1–13 (1965).
3. W. Larcher, *Physiological Plant Ecology. Ecophysiology and Stress Ecology of Functional Groups* (Springer-Verlag, ed. 4, 2003).
4. G. S. Campbell, J. M. Norman, *An Introduction to Environmental Biophysics* (Springer, ed. 2, 1998).
5. S. T. Michaletz et al., *Nat. Plants* **2**, 16129 (2016).
6. T. J. Givnish, *New Phytol.* **106** (suppl.), 131–160 (1987).
7. C. Körner, M. Neumayer, S. P. Menendez-Riedl, A. Smeets-Scheel, *Flora* **182**, 353–383 (1989).
8. S. Díaz et al., *Nature* **529**, 167–171 (2016).
9. D. M. Gates, *Annu. Rev. Plant Physiol.* **19**, 211–238 (1968).
10. A. Leigh, S. Sevanto, J. D. Close, A. B. Nicotra, *Plant Cell Environ.* **40**, 237–248 (2017).
11. D. F. Parkhurst, O. L. Loucks, *J. Ecol.* **60**, 505–537 (1972).
12. T. J. Givnish, G. J. Vermeij, *Am. Nat.* **110**, 743–778 (1976).
13. T. J. Givnish, in *Physiological Ecology of Plants of the Wet Tropics*, E. Medina, H. A. Mooney, C. Vázquez-Yanes, Eds. (Dr W Junk Publishers, 1984), pp. 51–84.
14. S. E. Taylor, in *Perspectives of Biophysical Ecology*, D. M. Gates, R. B. Schmerl, Eds. (Springer-Verlag, 1975), pp. 73–86.
15. B. F. Jacobs, *Palaeogeogr. Palaeoclimatol. Palaeoecol.* **145**, 231–250 (1999).
16. P. Wilf, S. L. Wing, D. R. Greenwood, C. L. Greenwood, *Geology* **26**, 203–206 (1998).
17. C. R. Fonseca, J. M. Overton, B. Collins, M. Westoby, *J. Ecol.* **88**, 964–977 (2000).
18. A. T. Moles et al., *J. Veg. Sci.* **25**, 1167–1180 (2014).
19. D. J. Peppe et al., *New Phytol.* **190**, 724–739 (2011).
20. D. Ackerly, C. Knight, S. Weiss, K. Barton, K. Starmer, *Oecologia* **130**, 449–457 (2002).
21. D. R. Greenwood, *Rev. Palaeobot. Palynol.* **71**, 149–190 (1992).
22. S. R. P. Halloy, A. F. Mark, *J. R. Soc. N. Z.* **26**, 41–78 (1996).

23. R. Leuning, *Agric. Meteorol.* **42**, 135–155 (1988).
24. D. N. Jordan, W. K. Smith, *Agric. Meteorol.* **71**, 359–372 (1994).
25. A. F. W. Schimper, *Plant Geography Upon a Physiological Basis* (Clarendon Press, 1903).
26. E. Warming, *Oecology of Plants* (Clarendon Press, 1909).
27. E. M. Curtis, C. A. Knight, K. Petrou, A. Leigh, *Oecologia* **175**, 1051–1061 (2014).
28. Z. H. Hu, Y. N. Xu, Y. D. Gong, T. Y. Kuang, *Photosynthetica* **43**, 529–534 (2005).
29. Y. Vitasse, A. Lenz, G. Hoch, C. Körner, *J. Ecol.* **102**, 981–988 (2014).
30. K. H. Jensen, M. A. Zwieniecki, *Phys. Rev. Lett.* **110**, 018104 (2013).
31. M. R. Raupach, *Q. J. R. Meteorol. Soc.* **127**, 1149–1181 (2001).
32. C. Huntingford, J. L. Monteith, *Boundary-Layer Meteorol.* **88**, 87–101 (1998).
33. N. Chiariello, in *Physiological Ecology of Plants of the Wet Tropics*, E. Medina, H. A. Mooney, C. Vázquez-Yanes, Eds. (Dr W Junk Publishers, 1984), pp. 85–98.
34. D. D. Ackerly, *Ecol. Monogr.* **74**, 25–44 (2004).
35. I. J. Wright, D. S. Falster, M. Pickup, M. Westoby, *Physiol. Plant.* **127**, 445–456 (2006).
36. U. Niinemets et al., *Ann. Bot.* **100**, 283–303 (2007).
37. M. Pickup, M. Westoby, A. Basden, *Funct. Ecol.* **19**, 88–97 (2005).
38. W. K. Smith, *Science* **201**, 614–616 (1978).
39. N. Dong, I. C. Prentice, S. P. Harrison, Q. H. Song, Y. P. Zhang, *Glob. Ecol. Biogeogr.* **26**, 998–1007 (2017).
40. L. Sack et al., *Nat. Commun.* **3**, 837 (2012).
41. A. T. Moles, M. Westoby, *Oikos* **90**, 517–524 (2000).
42. I. W. Bailey, E. W. Sinnott, *Science* **41**, 831–834 (1915).

ACKNOWLEDGMENTS

We thank the following people who generously provided access to previously unpublished trait data or data otherwise unavailable from source publications: D. Ackerly, H. Cornelissen, W. Cornwell, D. Duncan, E. Garnier, L. Yulin, J. Lloyd, H. Morgan, T. Navarro, J. Oleksyn, J. Overton, O. Phillips, N. Pitman, H. Poorter, L. Poorter, C. Vriesendorp, J. Wright, and A. Zanne. J. Cooke, T. Lenz, A. Ordonez, and J. Suitch helped compile and error-check trait data. This research was funded by the Australian Research Council (grants RN0459908, DP0558411, and FT100100910) and by Macquarie University (Ph.D. scholarship supporting N.D.) and is a contribution to the AXA Chair Programme in Biosphere and Climate Impacts and the Imperial College initiative on Grand Challenges in Ecosystems and the Environment. R.V. was funded by the Spanish Ministerio de Educación y Ciencia project ECO-MEDIT (CGL2014-53236-R) and European Fondo Europeo de Desarrollo Regional funds. B.F.J. acknowledges support from the National Science Foundation

(USA), grant EAR-9510015. This work originated from a working group held at Macquarie University. The leaf trait data set was compiled by I.J.W., E.A.L., and R.V.G., from literature data and data provided by S.D., R.V.G., B.F.J., R.K., M.R.L., Ü.N., P.B.R., R.V., M.W., P.W., and I.J.W. Geographic and climate data were compiled or calculated by I.J.W., E.A.L., V.M., and H.W. Statistical analyses were run by V.M. and I.J.W. The modeling component was conceived by I.C.P., N.D., and I.J.W. and run by N.D. L.S. initially suggested teaming empirical analysis with energy balance models. V.M., N.D., and R.V. created the figures. I.J.W. drafted the initial manuscript with assistance from I.C.P. All coauthors contributed to subsequent versions. The “global leaf size data set” is available as an Excel workbook in the supplementary materials.

SUPPLEMENTARY MATERIALS

www.sciencemag.org/content/357/6354/917/suppl/DC1
Materials and Methods
Figs. S1 to S13
Tables S1 to S4
References (43–181)
Data Set S1

26 November 2016; accepted 2 August 2017
10.1126/science.aal4760

Global climatic drivers of leaf size

Ian J. Wright, Ning Dong, Vincent Maire, I. Colin Prentice, Mark Westoby, Sandra Díaz, Rachael V. Gallagher, Bonnie F. Jacobs, Robert Kooyman, Elizabeth A. Law, Michelle R. Leishman, Ülo Niinemets, Peter B. Reich, Lawren Sack, Rafael Villar, Han Wang and Peter Wilf

Science **357** (6354), 917-921.
DOI: 10.1126/science.aal4760

Leaf size, climate, and energy balance

Why does plant leaf size increase at lower latitudes, as exemplified by the evolutionary success of species with very large leaves in the tropics? Wright *et al.* analyzed leaf data for 7670 plant species, along with climatic data, from 682 sites worldwide. Their findings reveal consistent patterns and explain why earlier predictions from energy balance theory had only limited success. The authors provide a fully quantitative explanation for the latitudinal gradient in leaf size, with implications for plant ecology and physiology, vegetation modeling, and paleobotany.

Science, this issue p. 917

ARTICLE TOOLS

<http://science.sciencemag.org/content/357/6354/917>

SUPPLEMENTARY MATERIALS

<http://science.sciencemag.org/content/suppl/2017/08/31/357.6354.917.DC1>

REFERENCES

This article cites 159 articles, 6 of which you can access for free
<http://science.sciencemag.org/content/357/6354/917#BIBL>

PERMISSIONS

<http://www.sciencemag.org/help/reprints-and-permissions>

Use of this article is subject to the [Terms of Service](#)



Supplementary Material for Global climatic drivers of leaf size

Ian J. Wright,* Ning Dong, Vincent Maire, I. Colin Prentice, Mark Westoby, Sandra Díaz, Rachael V. Gallagher, Bonnie F. Jacobs, Robert Kooyman, Elizabeth A. Law, Michelle R. Leishman, Ülo Niinemets, Peter B. Reich, Lawren Sack, Rafael Villar, Han Wang, Peter Wilf

*Corresponding author. Email: ian.wright@mq.edu.au

Published 1 September 2017, *Science* **357**, 917 (2017)
DOI: 10.1126/science.aal4760

This PDF file includes:

Materials and Methods
Figures S1 to S13
Tables S1 to S4
References

Other Supplementary Material for this manuscript includes the following:

(available at www.sciencemag.org/content/357/6354/917/suppl/DC1)

Data Set S1

Materials and Methods

Data compilation

Our leaf size data compilation is site-based; i.e., built from datasets describing non-agricultural vegetation to which we could reasonably assign geographic coordinates, and thus elevation and climate data. Sources of trait data included existing trait databases (43-45), relevant literature (journal articles, book chapters and published floras; from 1932 to present-day), and previously unpublished data provided by colleagues and coauthors of this article. “Leaf size” was defined as the one-sided projected area of mature, primary photosynthetic organs (including cladodes and phyllodes), measured on a projected-area basis. For compound-leaved species we considered leaflets as the primary photosynthetic organ (46), but also recorded the area of entire leaves, if known, and reported the latitudinal pattern for those data also. Note, the quantity that we refer to here as “leaf size” is also known as “leaf area” (8, 47-49).

Source studies varied in their underlying species-selection criteria. In some studies the species were chosen randomly; others considered the most abundant species only; many studies were restricted to particular growth forms or plant functional types (e.g., to woody species only), and some to particular taxonomic groups. Any data for seedlings and juvenile plants were excluded. Source studies also varied in how leaves were chosen. Quite commonly sampling was restricted to outer-canopy leaves, but in other cases leaves were chosen randomly, or without regard to canopy position or light exposure, or no information was given regarding leaf selection.

Various methods were used to measure leaf size. In more recent studies leaf area was typically measured using a flat-bed scanner. Methods from older studies included: use of a grid system such as a dot planimeter, or tracings on graph paper; weighed paper cut-outs; regressions on weight, length or width measurements – including species-specific regressions, site-specific regressions, and more generalized regressions such as length \times width adjusted by a correction factor for leaf shape (50), or length \times width by $2/3$ (51). In one literature lineage stretching back almost a century (46), species are assigned to leaf size categories (nanophyll, leptophyll, microphyll, mesophyll, macrophyll, megaphyll), with successive categories differing by a constant multiplier. For these datasets we assigned all species in a given category the geometric mean point of the category cut-offs. We included 1189 data rows of this type (*ca.* 8.5% of dataset). Given concerns about the potential for systematic underestimation of leaf area in such datasets (52) we ran preliminary analyses both with and without these data, but no qualitative effects were noted. Consequently these data were retained in the compilation and used in all final analyses.

Taxonomy. Taxonomic information was standardised as follows: angiosperm families follow the APG (Angiosperm Phylogeny Group) schema, ferns follow that of Smith *et al.* (53). Wherever possible, species names follow The Plant List (www.theplantlist.org; accessed May 2017).

Priority data types. Where, in a given study, multiple values of leaf size were reported for a given species from a given site, preference was given to data measured on outer-canopy (“sun”) leaves over data from inner- or lower-canopy “shade” leaves. Some sites occurred in more than one source dataset; where so, the datasets were merged. However, when the same species-site combination occurred in different studies, priority was given in relation to measurement type: direct measurement types (e.g. scanning or grid-based methods) were used in preference to indirect measurements (e.g. length by width calculations), and measurements made on samples were prioritized from those calculated from herbarium or flora data. Where samples with equivalent measurement types existed, these were given equal priority, and the data averaged. Finally, data were aggregated to mean leaf size values per species, for each of the 682 sites. For many sites source data were reported as species-at-site means, with no within-species information recorded, and so no aggregation was necessary. Conversely, this meant that we could not calculate uncertainty estimates associated with each species-at-site leaf size value.

Error checking. Various approaches were used to detect erroneous data. Graphical approaches included inspecting boxplots of leaf size from each site in relation to all other sites. For species with multiple data points we flagged any species that had conspicuously high maximum/minimum ratios, maximum-minimum sums, standard deviations, or coefficients of variation. Flagged species were checked one at a time, for data entry mistakes, and for unit errors – e.g. by comparison with data from published floras or online herbarium specimens. Corrections were made where possible. Some recurring cases of extreme variation for which valid reasons could be found were (1) Varying application of the definition of “leaf” or “leaflet”. (2) Measurement of ferns and other plants in which microclimate/growth conditions can produce notably variable leaf sizes. (3) Species with highly variable leaves such as (a) Herbs with morphologically different basal rosette and stem leaves; (b) Species with differing juvenile and mature leaves; (c) Species with extreme leaf heterogeneity (e.g. *Parsonsia heterophylla*).

Leaf type. Species were classified as having either simple or compound leaves based on information given in source publications, other trait databases; e.g., TRY (48), authoritative genus- or family-level descriptions (54), descriptions of individual species from relevant published and online floras and, as a last resort (but quite commonly), from images of leaves located via internet search engines. Data checking ensured internal consistency within the current dataset, but we assume that there must be some percentage of erroneous classifications. Note that we chose to follow a strict definition of “compoundness” (i.e., only including species with distinct leaflets), meaning that some modest number of species with functionally-compound, deeply-lobed leaves would have been classified as having simple leaves. Ferns and fern allies were considered somewhat differently: some were clearly simple-leaved, others clearly pinnate. In contrast to angiosperms, ferns with deeply divided, pinnatifid leaves were generally categorized as having compound leaves, as measurements usually only took in a portion of the frond (and because data were reported for pinnae by the original authors).

Life form. Species were described as being either woody or non-woody, or as having a particular growth form, based on information in source publications, floras, genus- or family-level descriptions (where appropriate), and from individual species descriptions. We defined growth forms as functional types not entirely constrained by phylogeny; for example *Xanthorrhoea* (monocot “grass trees”) were categorized as “shrubs”. “Graminoids” included true grasses (Poaceae) plus sedges (Cyperaceae), Restionaceae and Typhaceae (two species from each), Eriocaulaceae and Xyridaceae (one species from each). Each of these families is in Poales; but so too are Bromeliaceae (8 species; classified variously as herbs or epiphytes) and Flagellariaceae (one species with multiple occurrences, a vine). “Herbs” (or forbs) included non-graminoid herbaceous species. Climbing, twining and scrambling species were classified as “vines” if non-woody, and “lianas” if woody. Finally, “woody” species included all trees, shrubs, lianas and hemi-epiphytes, plus a small number of special cases, e.g. *Xanthorrhoea*, and palms (Arecaceae). “Non-woody” species included all graminoids, herbs, ferns, vines, succulents, and all epiphytes except *Poikilospermum suaveolens*, which is woody.

Phenology. Where possible, woody species were further classified as being deciduous or evergreen based on information available from the same data sources listed above for leaf type and life form. No information on phenology could be located for approximately 10% of woody species. We also attempted to classify all non-woody species as either annual, biennial or perennial, but were only able to locate information for *ca.* 40% of species, and so did not use this information further.

List of data sources for leaf size dataset

Previously unpublished or otherwise unavailable data were contributed by the authors of this article (SD, RK, MRL, RV, MW, PW, IJW) and by colleagues listed in Acknowledgments. Published data sources are listed in *References and Notes* as reference numbers 15, 17, 20, 37, 43-45, 69-178. All leaf size data used in our analyses are included in Database S1 (“Global leaf size dataset”).

Climate data

Location. Site locations (latitude, longitude) were taken from source publications or estimated from information given therein (WGS84 datum adopted as standard). Where published coordinates did not fall in the correct country or fell in water not on land (based on the climate raster layers), new coordinates were estimated (e.g. from Google Earth) based on site descriptions or simply moved to the nearest terrestrial suitable grid-cell on the Worldclim v1.3 raster layer (55), matching source and model elevation as best as possible. Site elevations were taken from source publications or, when unknown, by matching site coordinates to high-resolution digital elevation models underpinning the Worldclim v1.3 (55) and CRU CL2.0 (56) climatologies.

Climate data used for empirical analyses. As first preference we used temperature and precipitation data from source publications or from publicly available weather station data, where measured at the site itself (e.g. from biological station websites). Where climate was not known it was estimated from either Worldclim v1.3 (30 arc-second spatial resolution) or CRU CL2.0 (10' spatial resolution) following the rule-set:

- (a) Mean annual precipitation (MAP): if site elevation is already known, use precipitation data from the climatology which assumes the elevation most closely matching this known elevation. Otherwise, use Worldclim v1.3 by default.
- (b) Mean annual temperature (MAT): if both elevation and precipitation already known, use temperature data from climatology that best matches these (with stronger weighting on the match for precipitation). If only elevation known, use temperature data from climatology with closest matching assumed elevation, scaled if necessary using an altitudinal lapse rate of $-0.6^{\circ}\text{C}/100\text{m}$ (57).
- (c) Retrieve monthly temperature and precipitation trends from the respective climatology used for MAP or MAT. Scale monthly totals so that implied MAT or MAP matches that chosen in previous steps. That is, monthly temperatures were adjusted by the arithmetic difference between the model and original mean annual temperatures; monthly precipitation was adjusted by the proportional difference between the original and modelled annual precipitation.

Other climate variables retrieved from CRU CL2.0 were relative humidity (%) and the coefficient of monthly precipitation totals.

Solar radiation. Solar radiation was calculated following standard procedures (58, 59) to calculate top-of-atmosphere radiation from solar declination angle, and then top-of-canopy radiation following the Ångström-Preseott equation. This assumes that the optical thickness of air is constant over a wide range of latitudes and that 75% of top-of-atmosphere radiation reaches the canopy on completely sunny days, and 25% on completely cloudy days. Monthly mean fractional sunshine hours were derived from CRU CL2.0.

Moisture Index. A widely used moisture index (whether monthly or annual) is the ratio of precipitation to PET (potential evapotranspiration). There are various methods used for estimating PET. Here we use equilibrium evapotranspiration (ET_q) for this purpose, which is a function of net radiation and temperature only (59):

$$\lambda ET_q = R_n s / (s + \gamma) \quad (1)$$

where λ is the latent heat of vaporization of water (2.45 MJ/kg), R_n is net radiation (W m^{-2}), s is the slope of the Clausius-Clapeyron relationship (relating saturated water vapour pressure to temperature, evaluated at the ambient temperature; Pa K^{-1}) and γ is the psychrometer constant,

here taken as 65 Pa K^{-1} . Note, each of these constants show temperature and/or pressure dependencies, so more exact formulations are possible (58, 59). We calculated site Moisture Index (MI) as the ratio of summed annual precipitation to summed annual ET_q (or, when needed, on a growing season basis: see below). Temperature data were derived from CRU CL2.0. Net radiation was estimated from solar radiation following the approximations first described by Linacre (60) and adopted and evaluated in the SPLASH v1.0 program (59). The method yields estimates of the balance of net shortwave and net longwave radiation at the leaf surface during daytime, and of the (negative) net longwave radiation during night-time.

Growing Season. We defined the growing season as being the set of consecutive months that satisfied the conditions (61): (1) Monthly mean temperature $\geq 5^\circ\text{C}$ AND (2) Monthly precipitation / $ET_q \geq 0.05$. Exceptions were some very cold sites which by this definition would have no growing season at all: (i) “KornerMtWilhelm”. For this site no mean monthly temperatures satisfied criterion 1, but since the site is on a tropical mountain with an approximately aseasonal temperature pattern, we simply used data from all months as the “growing season”. (ii) “Moles Zackenberg Hill and Salix”. For this high latitude site no months satisfied criterion 1; here we defined growing season as being one month long (July, the warmest month).

Final list of climate variables. The final list of climate variables used, with abbreviations and units, was as follows: MAT: mean annual temperature ($^\circ\text{C}$); T_{CM} : mean temperature of coldest month ($^\circ\text{C}$), T_{WM} : mean temperature of warmest month ($^\circ\text{C}$); T_{gs} : mean temperature during growing season ($^\circ\text{C}$); T_{CMgs} : mean temperature of coldest month during the growing season ($^\circ\text{C}$); cvPPT: coefficient of variation of monthly precipitation (mm); RHann: mean annual daytime relative humidity (%); RHgs: mean daytime relative humidity during the growing season (%); ET_q : annual equilibrium evapotranspiration (mm); ET_{qgs} : growing season equilibrium evapotranspiration (mm); RADann: annual mean daily irradiance, annual (W m^{-2}); RADgs: growing season mean daily irradiance (W m^{-2}); MAP: mean annual summed precipitation (mm); PPTgs: mean growing season summed precipitation (mm); MIann: annual moisture index (mm mm^{-1}); MIgs: growing season moisture index (mm mm^{-1}).

Statistical analyses.

This study is a *data synthesis*: the leaf size data come from many studies, each with their own individual research question, and in our analysis the data are being fused and applied to a new question. It is in the nature of global data syntheses that the sampling is not random. It is theoretically possible to investigate the non-randomness in relation to any particular variable, but not possible to investigate in relation to all possible variables, or adjust for the non-randomness in any comprehensive way. We believe that the more conservative approach is to accept the non-randomness in the available data, and to assess it in relation to any particular conclusion -- is

there reason to think the conclusion could be an artefact of the non-randomness? For example, above we describe analyses that confirmed that including data from studies that used leaf size categories, rather than a continuous scale, did not affect the conclusions of the study.

Analyses. Leaf size data were log-transformed for analyses, both for statistical reasons (transformation corrected the right-skew and approximately equalized variance in relation to the mean) and for logical reasons: it makes more sense to consider size-related biological variables on a multiplicative scale rather than on an arithmetic scale (62). Strongly right-skewed climate variables (MAP, MI, MIgs, MAPgs) were also log-transformed.

Global geographic patterns in leaf size are expected to reflect both the different ecological competences that distribute species with different leaf sizes selectively across environments in the present day, and also phylogenetically-conserved differences between major clades in leaf size and habitat preference. (These are complementary rather than competing accounts). In this study we focus on present-day competence, noting taxonomic patterning along the way.

Relationships between leaf size, latitude and climate were quantified using linear mixed regression models using the R package *lme4*, which fits models based on restricted maximum likelihood. We treated climate variables as fixed effects, site as a random effect (to account for site-to-site variation not explained by climate variables), and species as a random effect (because many species occurred multiple times in the database, at different sites). We note that, by including site as a random effect, spatial autocorrelation in model residuals was rendered non-significant in key analyses such as Fig. 2 (leaf size as a function of MAP, T_{WM} and their interaction; spatial analyses not shown).

For these linear mixed models we calculated r^2 values following Moles et al. (63). Those authors partitioned r^2 into the component explained by site climate (using the reduction in residual sum of squares on inclusion of fixed effects only), the between-site component that remained unexplained (using the change in residual sums of squares on inclusion of random effects terms), and the within-site component (i.e., the remaining unexplained variation). Here we report just the first of these three possible values, since our primary interest was in the explanatory power of site climate. That is, the r^2 values are identical to those calculated in analyses incorporating fixed effects only (or nearly so). By contrast, the fitted coefficients differ from those that would be calculated using models with fixed effects only, because we included the site and species random effects. Standard assumptions of linear regression were made for the reported analyses (homogeneity of variance, approximately normal distribution of data and residuals).

When exploring interactive climate effects on leaf size (e.g. Fig. S5) we coded species into categories based on MAP, RADann and T_{WM} , largely for purposes of illustration. While we considered the primary results to be the multiple regression equations reported in the figure caption, the group-coded analyses better emphasized the finding that relationship r^2 values were higher among wetter, hotter and higher irradiance sites. In choosing group definitions, for each variable we chose several sets of category cut-off points, both by splitting the data into 4-5

equally-sampled groups (e.g. for MAP, Figs S6A,B), and by defining 4-5 groups with equal bin-width (e.g. for T_{WM} , and RADann; Figs S6C,D). The choice of bin-type made no qualitative difference to the results. Consequently, we used a mixture of equally-sampled and equal-width types.

Modelling leaf energy budgets

The leaf energy balance is classically represented as a function of net radiation, air temperature, stomatal and boundary-layer conductances and vapour pressure deficit (2, 4). Optimality treatments for leaf size have varied these factors one at a time (sometimes in a factorial design) and quantified their effects on photosynthesis and transpiration, or their ratio (water-use efficiency), or the arithmetic difference of their unit costs (2, 9, 11-14, 33, 64, 65). We apply a reduced form of the standard energy balance calculation making use of the Priestley-Taylor approximation for evapotranspiration (ET), which can be derived from boundary-layer theory (31, 32). This approximation states that total ecosystem evapotranspiration (ET) under well-watered field conditions is approximately proportional to ET_q as defined above, the constant of proportionality (α_0) commonly being taken as 1.26 (66) although there is some (observed and predicted) variation around this value. The product of ET_q and α_0 (hereafter, PET_q) is a practical and widely used definition of PET. It can be interpreted as representing the atmospheric demand for ET, and as such it is independent of leaf and canopy conductances. Under well-watered conditions, actual ET is well approximated by the Priestley-Taylor potential rate. However, as water supply declines, stomatal closure and (where relevant) leaf shedding progressively reduce ET (32). We have assumed that well-watered plants transpire at this potential rate, and that this rate is reduced by a factor $\kappa = (\alpha/\alpha_0)^{1/4}$, where α is the monthly Cramer-Prentice moisture index (67) calculated as in SPLASH v1.0 (59), and $\alpha_0 = 1.26$.

The steady-state temperature of leaves (which is reached within minutes) is determined by the necessary equality between the net radiation at the leaf surface and the sum of sensible and latent heat exchanges with the surrounding air, the former being proportional to the leaf-to-air temperature difference (ΔT), the latter to the transpiration rate. Whether ΔT is negative or positive, its magnitude depends on the leaf boundary-layer conductance (g_b). Small leaves are highly coupled to the atmosphere, i.e. they have a large g_b . Larger leaves are less well coupled to the atmosphere, i.e. they have a smaller g_b and so tend to have a larger (negative or positive) ΔT . By specifying lower and upper thermal limits for leaf damage one can predict the maximum leaf size in any given climate as the smaller of two predicted values, one based on the night-time constraint (the risk of frost damage), the other on the daytime constraint (the risk of overheating). The former is calculated based on the night-time (negative) R_n and the mean minimum temperature of the coldest month with a mean temperature $> 0^\circ\text{C}$. The latter is calculated based on the R_n at solar noon of the warmest month and the mean maximum temperature of the warmest month. The steady-state energy balance equation used for these calculations is (in molar units):

$$\Delta T = (R_n - \lambda E)/(c_p g_b) \quad (2)$$

where λ is the latent heat of vaporization of water, $E = \alpha_0 \kappa ET_q$, and c_p is the heat capacity of air (1013 kg K^{-1}). ΔT is negative at night (when R_n is negative and $\lambda E = 0$), and in the day when $\lambda E > R_n$ – a situation that commonly occurs under conditions of high temperature and vpd.

Equation (2) can be solved for the value of g_b that yields a temperature ($T + \Delta T$, where T is the ambient temperature considered) equal to the (low or high) lethal temperature. We have taken these temperatures to be -5°C (29) and 50°C (27, 28), respectively. In turn, we derive the leaf size corresponding to this value of $g_b(I)$, using:

$$g_b = 0.00662 \sqrt{(u/d)} \quad (3)$$

and

$$A_L = 1.5 d^2 \quad (4)$$

where g_b is in units m s^{-1} , u is wind speed (we have used a nominal value of $u = 0.1 \text{ m s}^{-1}$: a low value since the largest ΔT occur under still conditions), d is the characteristic dimension of the leaf (m), and A_L is the area of the leaf (m^2).

Fig. 3 shows latitudinal trends in maximum leaf size as predicted by modelling leaf energy budgets. As described above, for each of the 682 sites in the leaf size dataset we generated two sets of predictions of maximum potential leaf size, one based on daytime constraints, one on night-time constraints. For each set we created 2-degree width latitude bins and calculated the median leaf size value for each bin, then we illustrated the general trend through these values using LOESS regression (implemented using the standard function in *R*, using the default value 0.66 for the smoothing parameter). Sites where the daytime prediction was for infinite leaf size were assigned the arbitrarily large value $10^{0.5} \text{ m}^2$, so that the data were still included in the LOESS regression. The latitudinal trend based on daytime constraints is illustrated using a red-dashed line; that based on night-time constraints uses a blue-dashed line. Calculations using alternative values of key parameters resulted in slight upward or downward shifts of the curves relating predicted maximum leaf sizes to latitude, without altering their general form (Figs S9-S12).

Fig. 4 shows predicted global patterns in maximum leaf size. Calculations were made using the same approach as for the site-specific analysis (and with low and high lethal temperatures of -5°C and 50°C , respectively, and wind-speed of 0.1 m s^{-1}), but using climate data from the CRU TS 3.24 dataset (68) for every terrestrial grid cell (0.5 degree spatial resolution). In Fig. 4 each cell is color-coded according to the final (i.e., smaller) of the two predictions for maximum leaf size (one for night-time, one for daytime). We assigned an arbitrarily large value of $10^{0.5} \text{ m}^2$ to cells where the final prediction indicated no effective thermal constraint (i.e., infinite size).

predicted from daytime calculation; unfeasibly large leaves predicted from night-time prediction).

Fig. S13 indicates for each grid cell whether the smaller prediction was derived from the night-time or daytime calculation, whether the two values were of similar magnitude (“co-limited”), or whether there was no effective thermal limit (“unlimited”). Co-limitation was assigned to grid cells where the ratio of the night- and daytime predictions for maximum leaf size fell between 0.5 and 2.0. “Unlimited” cells were those where the final prediction for maximum leaf size was $> 10^{0.477} \text{ m}^2$ (i.e. $> 3 \text{ m}^2$), which corresponds to the deepest shade of blue in Fig. 4. In Fig. S13 the total land area represented by night-limited, day-limited, co-limited and unlimited grid cells was calculated by projecting to a cylindrical equal-area projection, in which each grid cell represents 2311 km^2 of land area and there are 58051 cells ($134,155,861 \text{ km}^2$ of land area). On that basis, 51 % of land area was included in the night-limited category, 38 % in the day-limited category, 6.7 % was designated as co-limited and 4.3 % as unlimited.

Our method could be applied to other locations of interest by following the approach outlined above (Equations 1-4 and accompanying text). To run SPLASH v1.0 (59) one needs information on latitude, elevation, monthly mean temperatures, monthly precipitation, and monthly cloudiness (or sunshine fraction, from which cloudiness can be estimated). In addition, mean monthly values of the daily maximum temperature are required for calculating daytime-limited maximum leaf size, and mean monthly values of the daily minimum temperature are required for calculating night-limited maximum leaf size. All of these variables can be found in CRU climate datasets (56,68), but the same approach could be used at higher spatial resolution by using appropriate climate data from any reputable source.

Supplementary Figures

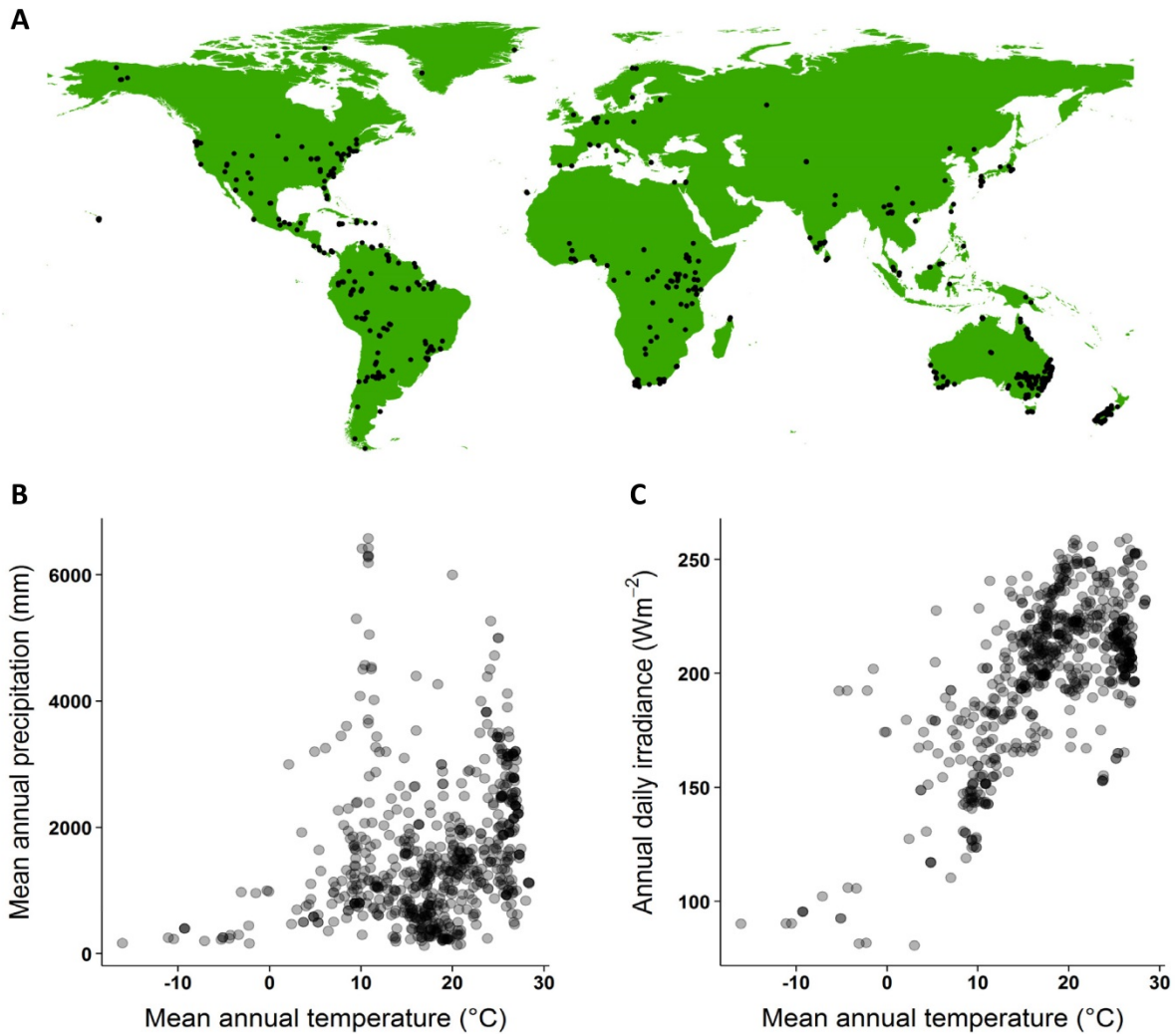


Figure S1. Locations and basic climate information for the 682 study sites.

(A) World map showing geographical location of each site. (B) Position of the study sites in MAP – MAT climate space. (C) Position of the study sites in irradiance – MAT climate space. Where data points overlap in panels (B) and (C) this is indicated with darker shading.

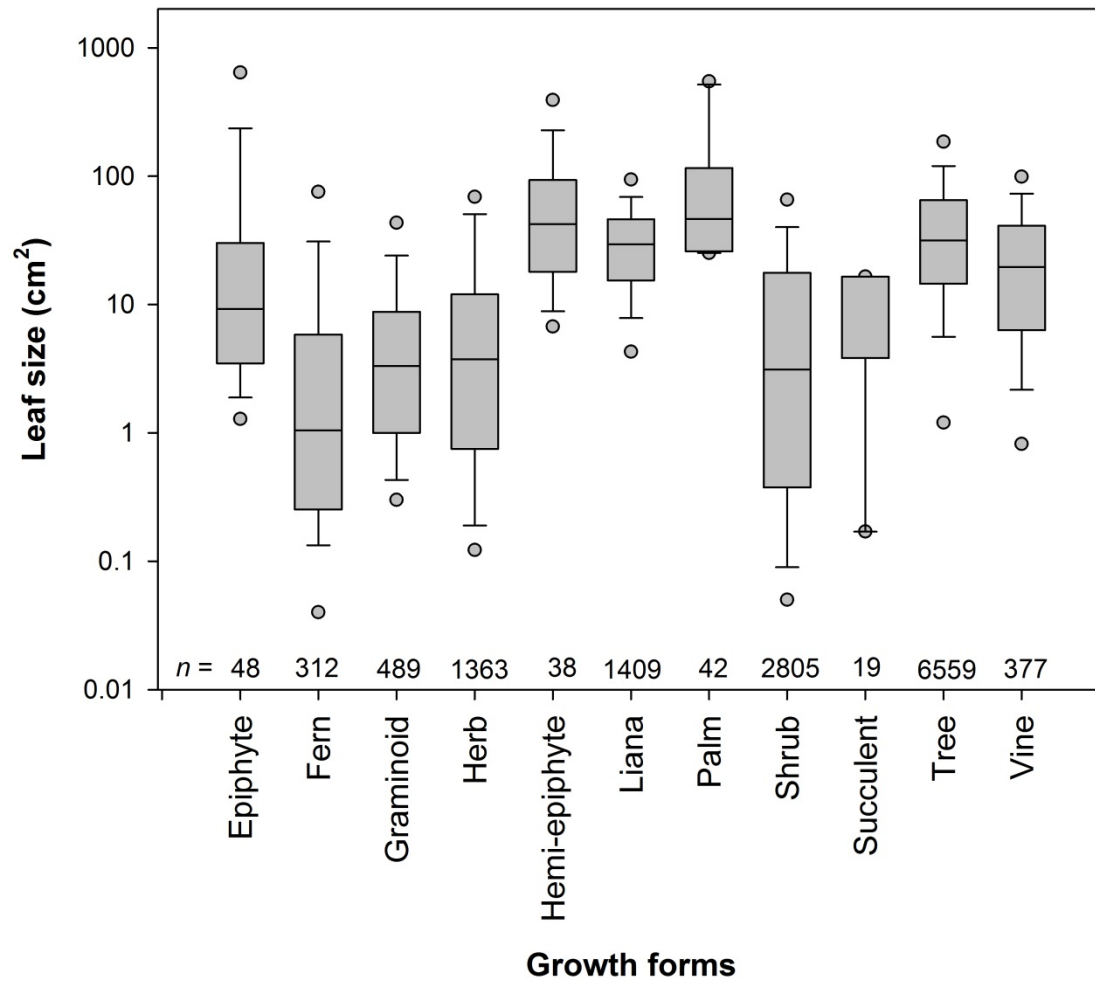


Figure S2. Box-and-whisker plots of leaf size with species categorized by common growth forms.

Boxes indicate the interquartile range, whiskers the 5th and 95th percentiles, the full line is the median. Numbers of species-at-site mean values per growth form are shown at the bottom of the figure. Note: “Herb” refers to herbaceous dicots (or forbs). Climbing and twining species were divided into herbaceous and woody species-groups (“vines” and “lianas”, respectively).

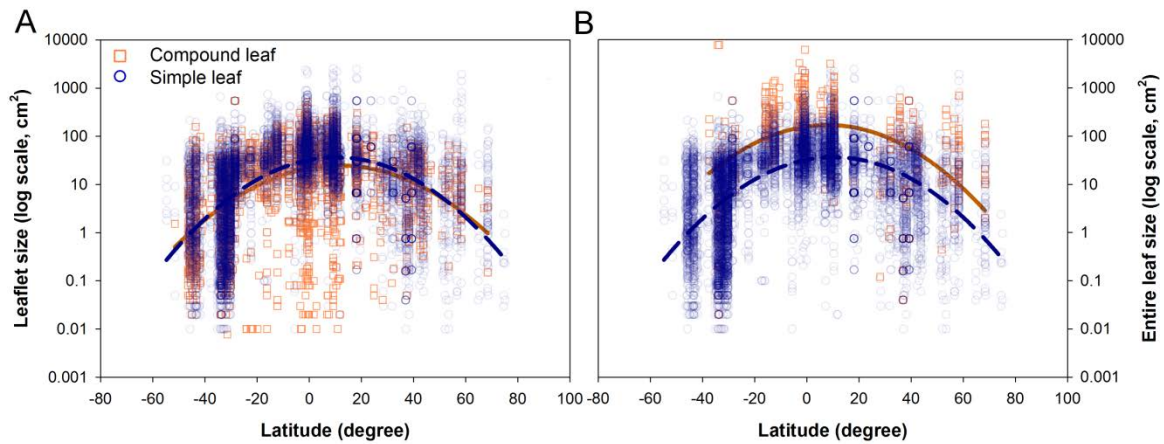


Figure S3. Leaf size – latitude relationships for simple- and compound-leaved species considered separately.

For compound-leaved species we primarily defined “leaf” size as the average size of individual leaflets (panel **A**), but also considered the latitudinal trend with leaf size redefined as that of entire leaves (panel **B**). Note the very similar results for both leaf-types, and the approximately constant offset between trends for simple-leaved and compound-leaved species when considering leaf size of compound-leaved species as that of the entire leaf.

Equations, panel (**A**). Compound-leaved (leaflets):

$$\text{LogLS} = 1.22 + 0.006 \text{ Lat} - 0.0003 \text{ Lat}^2, r^2 = 0.21, n = 2523, P < 0.0001.$$

$$\text{Simple-leaved: } \text{logLS} = 1.39 + 0.009 \text{ Lat} - 0.0004 \text{ Lat}^2, r^2 = 0.29, n = 10940, P < 0.0001.$$

Equations, panel (**B**). Compound-leaved (entire leaves):

$$\text{LogLS} = 2.13 + 0.006 \text{ Lat} - 0.0005 \text{ Lat}^2, r^2 = 0.18, n = 519, P < 0.0001.$$

Simple-leaved: same equation as in panel **A**.

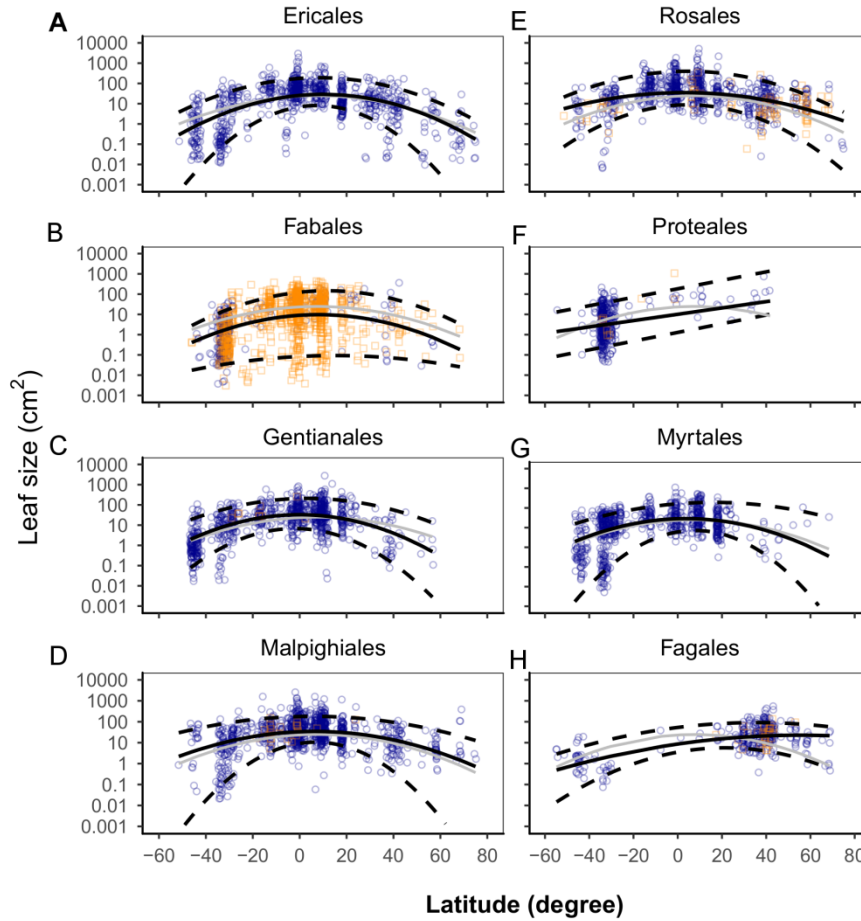


Figure S4. Leaf size – latitude relationships for selected taxonomic orders.

Panels **A** to **E** show data for the orders most strongly represented in our dataset: Ericales (891 species-at-site mean values), Fabales (1147 values), Gentianales (934 values), Malpighiales (1163 values), Rosales (830 values). Panels **F** to **H** show data for three orders with markedly non-cosmopolitan distributions (Proteales and Myrtales: predominantly southern hemisphere; Fagales: bimodal). Species are coded as simple-leaved (blue circles) or compound-leaved (orange squares; for which “leaf” size refers to that of the leaflets). Solid fitted lines correspond to quadratic mixed regressions for all species (grey lines) and specific plant orders (black lines). Dashed lines show the 5th and 95th quantile quadratic regression fits. Details of quadratic mixed regressions:

Ericales: $\log LS = 1.41 + 0.011 \text{ Lat} - 0.0005 \text{ Lat}^2$, $P < 0.001$, $r^2 = 0.46$

Fabales: $\log LS = 0.98 + 0.008 \text{ Lat} - 0.0005 \text{ Lat}^2$, $P < 0.001$, $r^2 = 0.23$

Gentianales: $\log LS = 1.52 - 0.0002 \text{ Lat} - 0.0006 \text{ Lat}^2$, $P < 0.001$, $r^2 = 0.47$

Malpighiales: $\log LS = 1.52 + 0.005 \text{ Lat} - 0.0004 \text{ Lat}^2$, $P < 0.001$, $r^2 = 0.25$

Rosales: $\log LS = 1.55 + 0.002 \text{ Lat} - 0.0003 \text{ Lat}^2$, $P < 0.001$, $r^2 = 0.26$

Proteales: $\log LS = 1.00 + 0.016 \text{ Lat}$, $P < 0.001$, $r^2 = 0.17$

Myrtales: $\log LS = 1.45 + 0.004 \text{ Lat} - 0.0005 \text{ Lat}^2$, $P < 0.001$, $r^2 = 0.29$

Fagales: $\log LS = 0.94 + 0.015 \text{ Lat} - 0.0001 \text{ Lat}^2$, $P < 0.001$, $r^2 = 0.48$

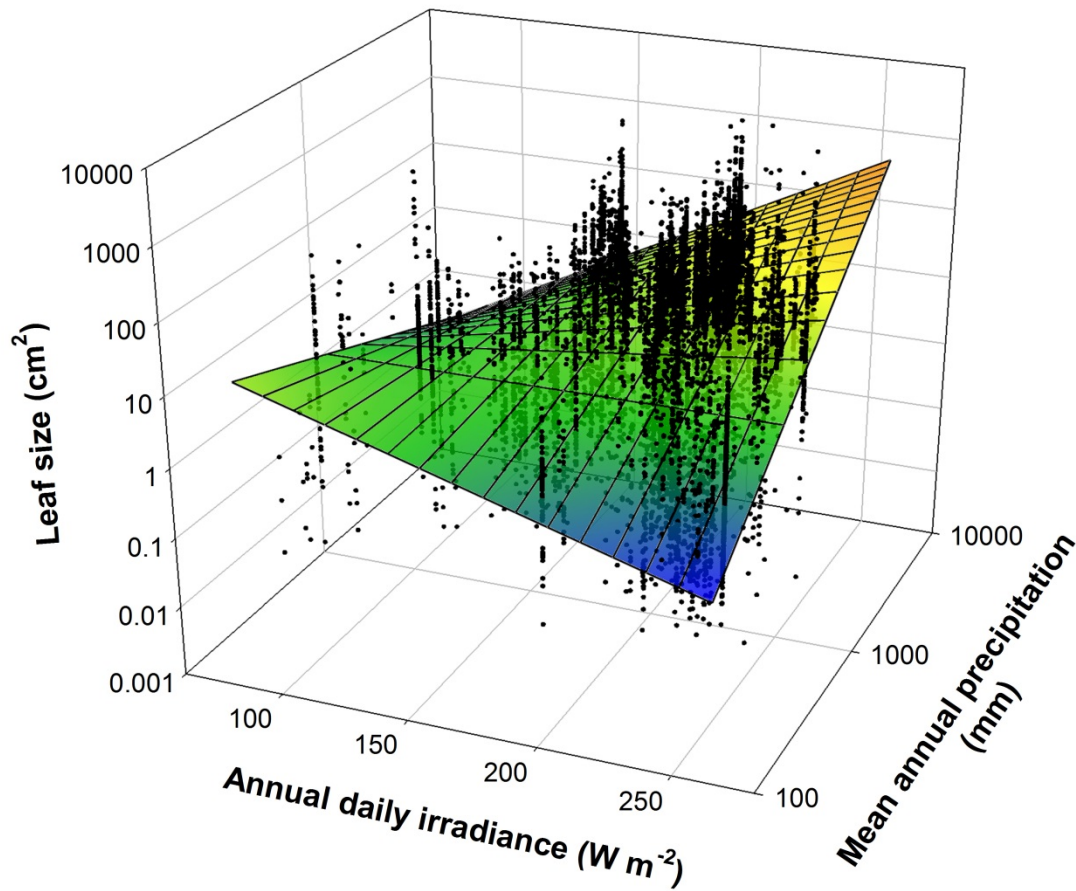
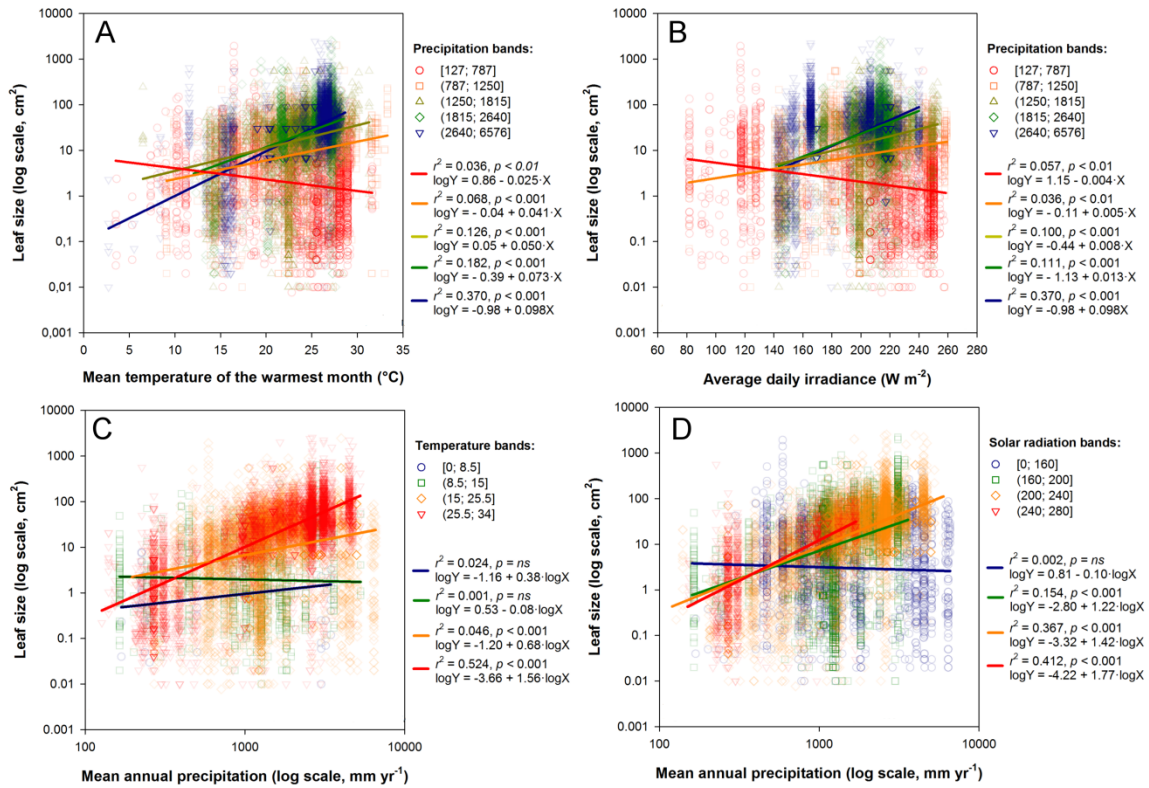


Figure S5. Global variation in leaf size as a function of site irradiance and precipitation.

Considering leaf size (LS) as a function of mean annual daily irradiance (RAD) and mean annual precipitation (MAP), the best-fit surface estimated by multiple mixed-model regression was a twisted plane with the form:

$$\log LS = -0.05 \text{ RAD} - 2.23 \log \text{MAP} + 0.02 \text{ RAD} \times \log \text{MAP} - 6.70 \text{ (all parameters } P \ll 0.001; r^2 = 0.29, N = 13641).$$



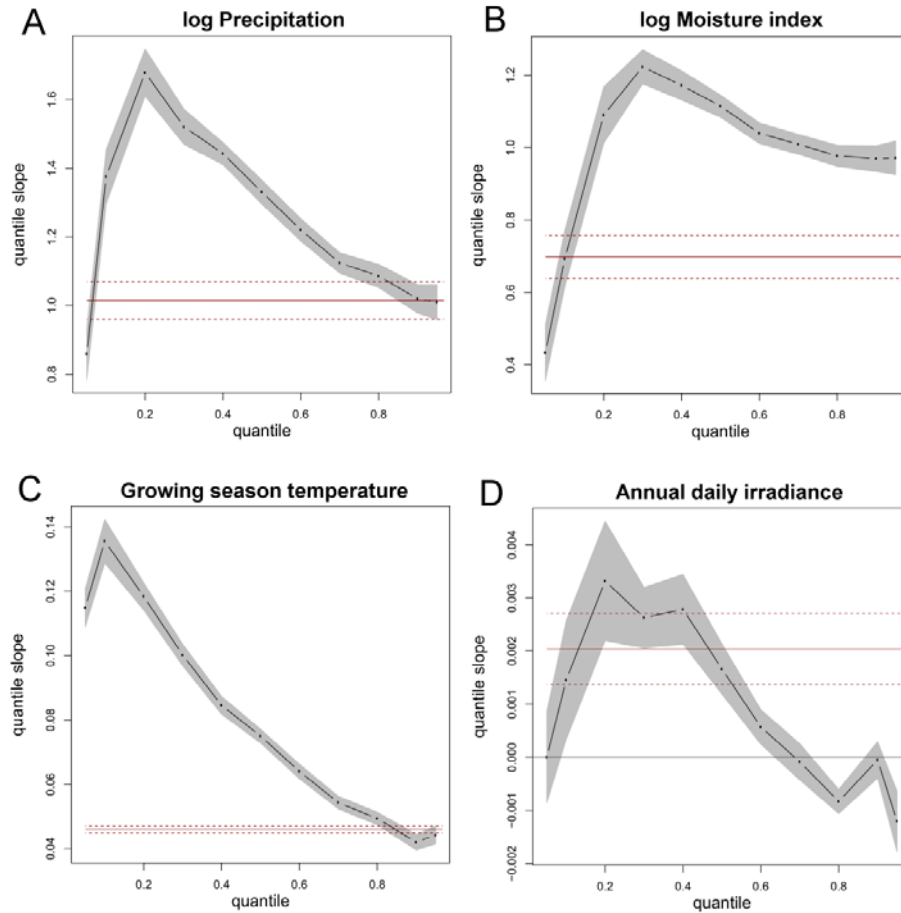


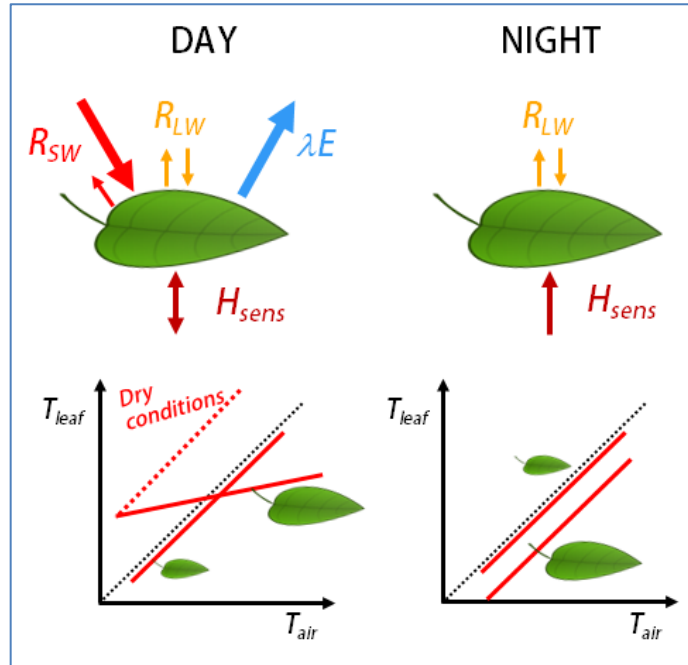
Figure S7. Trends in quantile regression slopes fitted to various quantile ranges of the data clouds depicted in Figs. 1B-E (relationships between leaf size and key climate variables).

Climate variables: **A**: mean annual precipitation; **B**: moisture index (annual mean); **C**: mean temperature during the growing season; **D**: daily solar radiation, annual mean. Quantile regression slopes and 95% confidence intervals were calculated using the *quantreg* package in R. For informal comparison purposes only, the slope and 95% confidence intervals from linear mixed model regressions are shown on each panel in red.

Figure S8. Illustration of key points in the leaf energy balance model

In our simplified leaf energy balance model the only fluxes that we consider are (a) the net radiation at the leaf surface (R_n ; itself the balance of shortwave R_{SW} and longwave R_{LW} fluxes) (b) sensible heat fluxes (H_{sens}), and (c) latent heat flux (from transpiration; λE). The relative magnitudes of fluxes during day and night are indicated by arrow sizes. We assume steady-state conditions and ignore several minor processes included in full models of leaf energy balance (e.g. (1, 9)), including the long-wave radiation (R_{LW}) emitted by the ground and absorbed by the leaf, and the small effect on long-wave radiation emitted from the leaf when $\Delta T \neq 0$. ΔT is the difference between leaf and air temperatures, indicated by the vertical displacement from the 1:1 black dotted line in the graphs.

Daytime. R_n is positive, the chief contributor being short-wave radiation from the sun (R_{SW}). The sign of ΔT depends on the balance of R_n and λE , which can exceed R_n at high temperatures, implying a negative sensible heat flux. The magnitude of ΔT depends on the leaf boundary-layer conductance (g_b). At a given wind-speed smaller leaves have a thinner boundary layer and so larger g_b . Consequently the temperature of small leaves tends to closely track that of the surrounding air.



By contrast, larger leaves have a thicker boundary layer and a smaller g_b , and so tend to have a larger ΔT , whether negative or positive. Under mid-day, warm, well-watered conditions, large-leaved species may exhibit positive ΔT at low T_{air} and negative ΔT at high T_{air} (4, 39, 179). However, when low soil moisture limits transpiration and the air is warm, T_{leaf} may become damagingly high (red dashed line, indicating large ΔT).

Night-time. Smaller leaves have larger g_b , meaning that their T_{leaf} closely tracks T_{air} (the magnitude of ΔT is only ever small). The lower g_b of larger leaves hinders sensible heat exchange. Consequently, under clear night-time skies T_{leaf} may become damagingly low even if T_{air} is several degrees above freezing (23, 24, 180, 181). This tendency is strongly affected by wind-speed: on windy nights the boundary layers of leaves are sufficiently disrupted that frost damage rarely occurs.

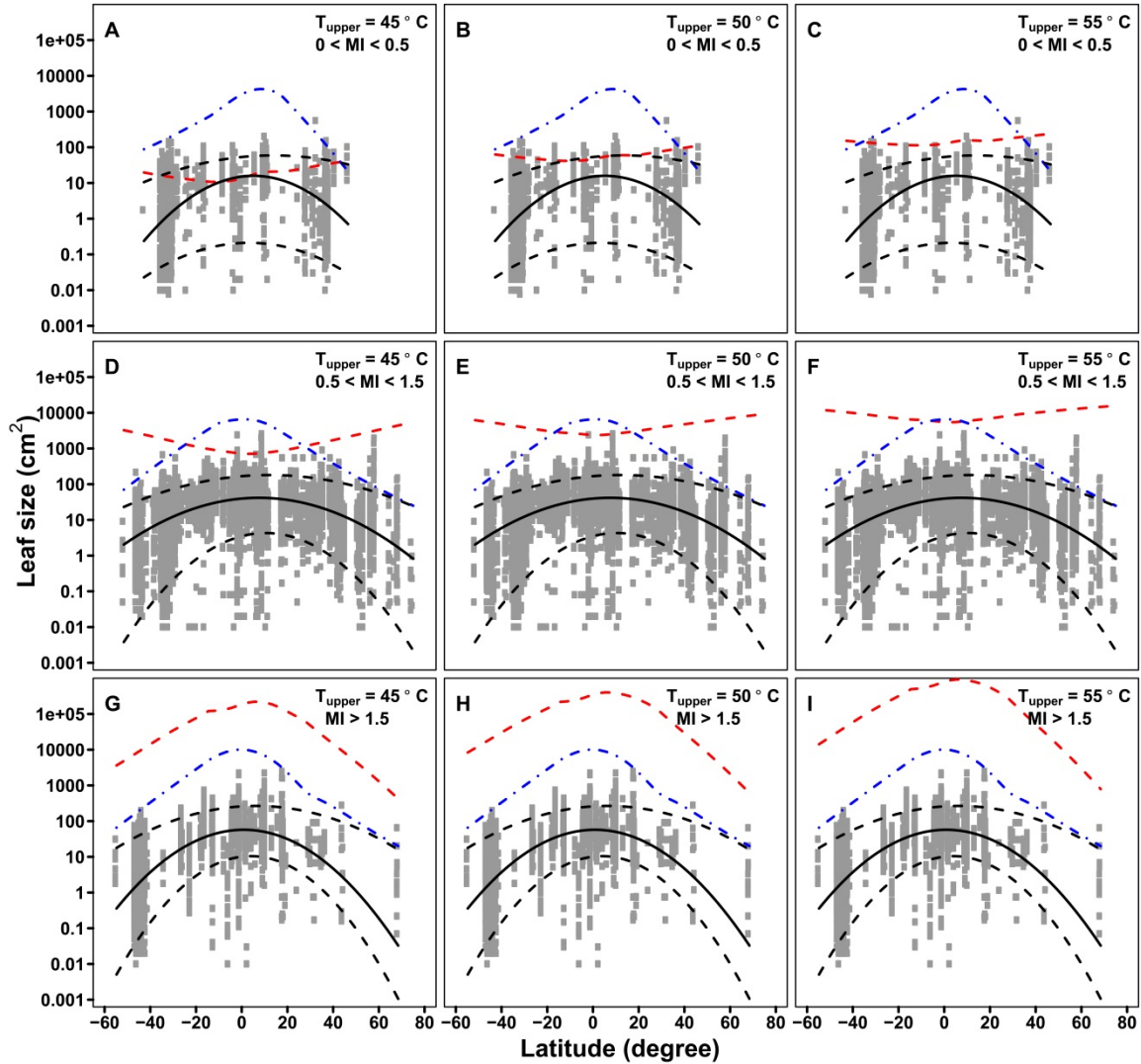


Figure S9. Effect of varying the upper lethal temperature when modelling daytime constraints on maximum leaf size (risk of over-heating).

In the main results (Figure 3) the upper lethal temperature was set to 50 °C (reproduced here as the middle column of panels). Here we show that the effect of choosing either 45 °C (left column) or 55 °C (right column) for this parameter is mostly to decrease or increase the elevation of the median prediction line (red dashes), with little or no difference made to its general form. As in the main results the dataset is subdivided by annual moisture index (panels **A-C**, $0 < \text{MI} < 0.5$; **D-F**, $0.5 < \text{MI} < 1.5$; **G-I**, $\text{MI} > 1.5$), with mean and 5th/95th quantile quadratic regressions shown in black (solid and dashed lines, respectively).

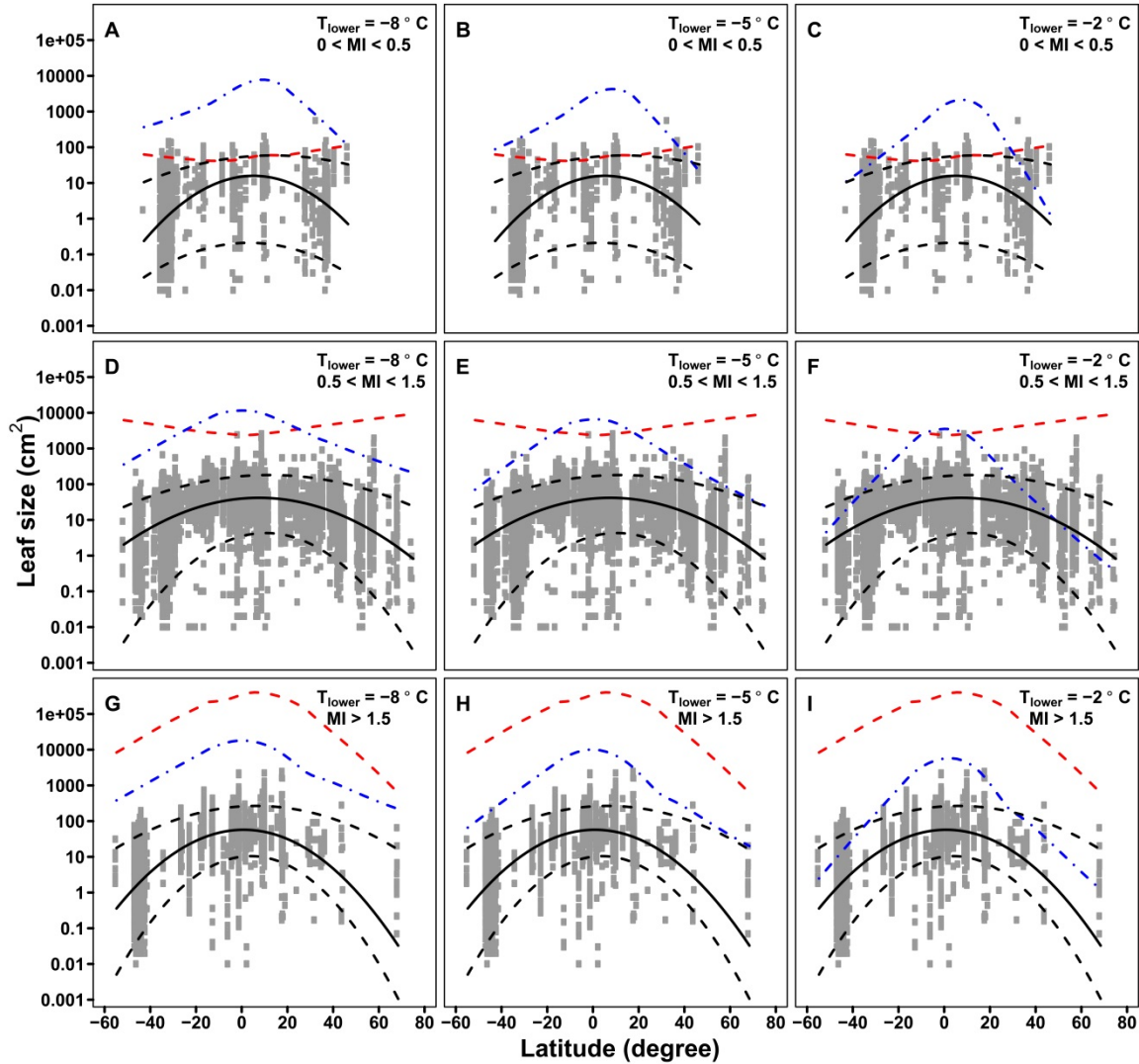


Figure S10. Effect of varying the lower lethal temperature when modelling night-time constraints maximum leaf size (risk of frost-damage).

In the main results (Figure 4) the lower lethal temperature was set to -5°C (reproduced here as the middle column of panels). Here we show that the effect of choosing either -8°C (left column) or -2°C (right column) for this parameter is mostly to decrease or increase the elevation of the median prediction line (blue dashes), especially at high latitudes. As in the main results the dataset is subdivided by annual moisture index (panels **A-C**, $0 < \text{MI} < 0.5$; **D-F**, $0.5 < \text{MI} < 1.5$; **G-I**, $\text{MI} > 1.5$), with mean and 5th/95th quantile quadratic regressions shown in black (solid and dashed lines, respectively).

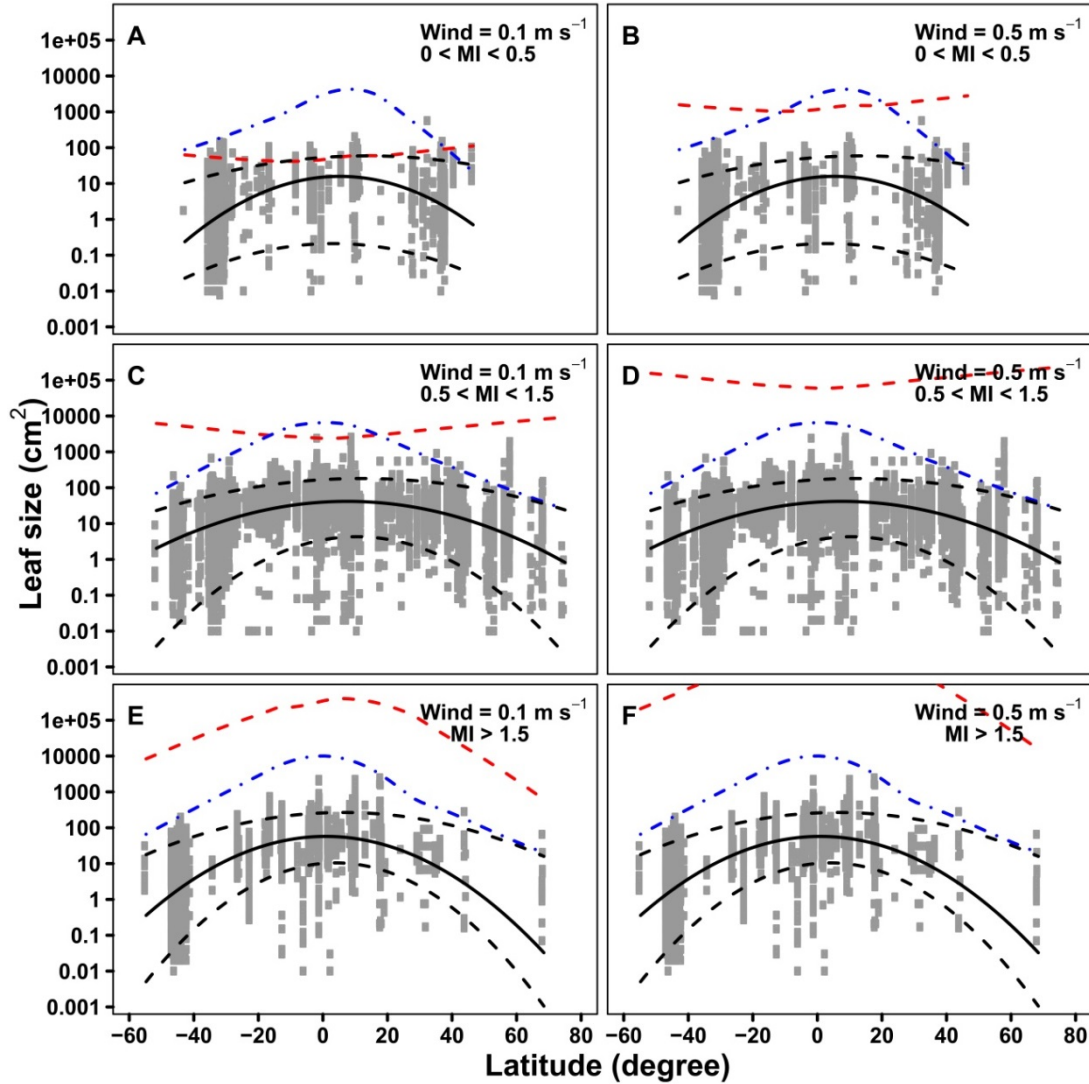


Figure S11. Effect of varying daytime wind speed when modelling daytime constraints on maximum leaf size (risk of over-heating).

In the main results (Figure 3), daytime wind-speed was set to 0.1 m s^{-1} (reproduced here as the left-hand set of panels). Here we show that the effect of choosing a higher wind-speed (which has the effect of disrupting the leaf boundary layer) is simply to predict far larger possible leaf sizes at any given latitude, based purely on daytime considerations (red dashed lines, right-hand panels). As in the main results the dataset is subdivided by annual moisture index (panels **A-B**, $0 < \text{MI} < 0.5$; **C-D**, $0.5 < \text{MI} < 1.5$; **E-F**, $\text{MI} > 1.5$), with mean and 5th/95th quantile quadratic regressions shown in black (solid and dashed lines, respectively).

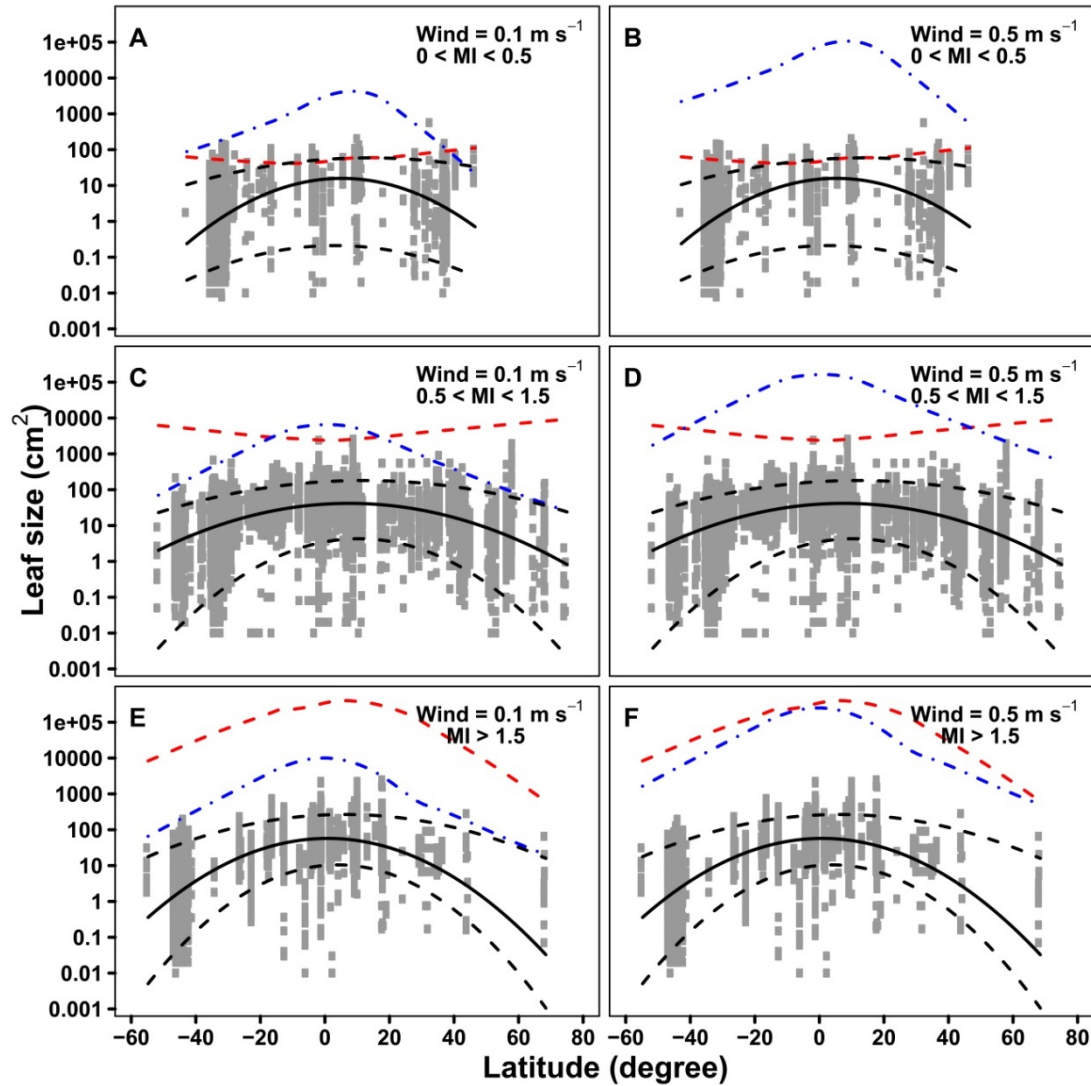
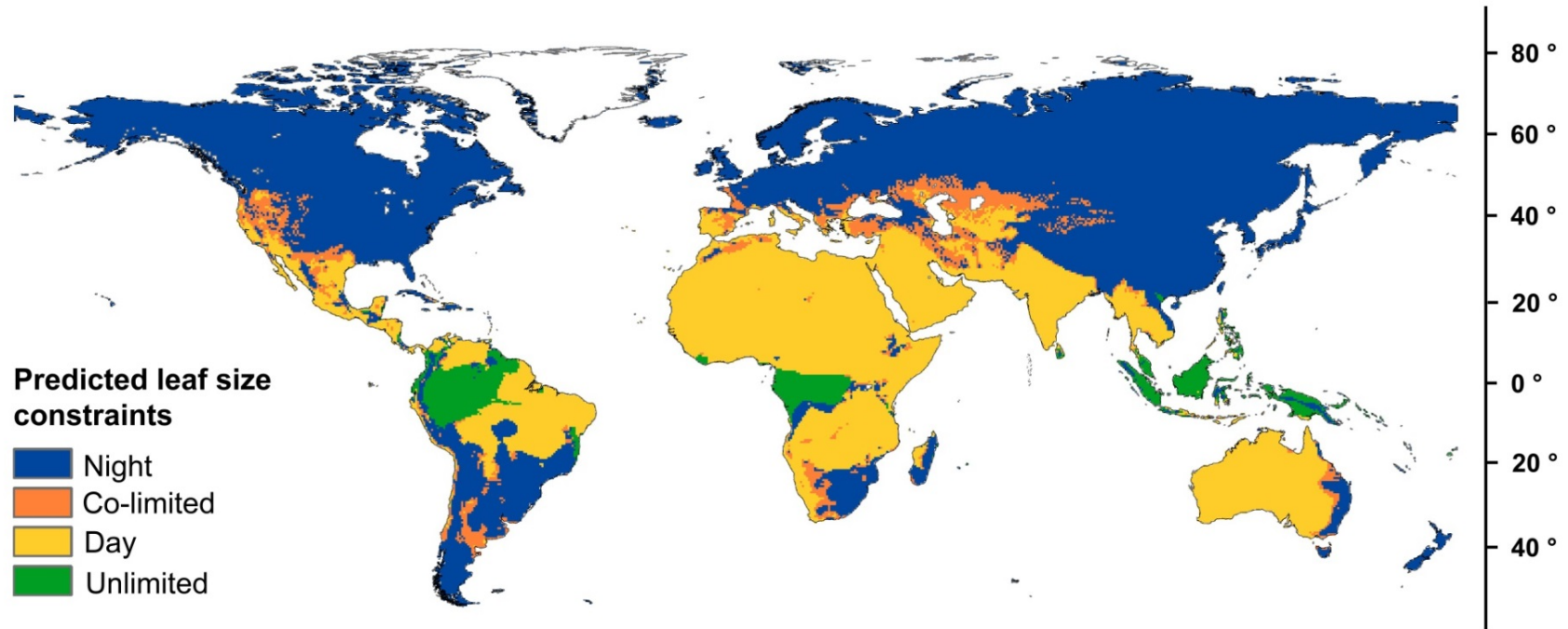


Figure S12. Effect of varying night-time wind speed when modelling night-time constraints on maximum leaf size (risk of night-chilling).

In the main results (Figure 3), night-time wind-speed was set to 0.1 m s^{-1} (reproduced here as the left-hand set of panels). Here we show that the effect of choosing a higher wind-speed (which has the effect of disrupting the leaf boundary layer) is simply to predict far larger possible leaf sizes at any given latitude, based purely on night-time considerations (blue dashed lines, right-hand panels). As in the main results the dataset is subdivided by annual moisture index (panels **A-B**, $0 < \text{MI} < 0.5$; **C-D**, $0.5 < \text{MI} < 1.5$; **E-F**, $\text{MI} > 1.5$), with mean and 5th/95th quantile quadratic regressions shown in black (solid and dashed lines, respectively).

Figure S13. Global map indicating the basis for the prediction of maximum leaf sizes in Fig. 4.

Each grid cell is color-coded so as to indicate whether the final (i.e., smaller) of the two predictions for maximum leaf size was based on daytime conditions (risk of over-heating, evaluated at solar noon of the warmest month of the year), on night-time conditions (risk of frost damage, evaluated for the coldest month with a mean temperature $> 0^{\circ}\text{C}$), on both day and night conditions approximately equally (“co-limited”), or whether there was no effective thermal limit on leaf size (predicted maximum leaf size $> 3 \text{ m}^2$; “unlimited”). Co-limitation was assigned to grid cells where the ratio of the day and night predictions for maximum leaf size fell between 0.5 and 2.0.



Supplementary Tables

| | MAT | T _{CM} | T _{WM} | T _{gs} | T _{CMgs} | cvPPT | RHann | RHgs | ET _q | ET _{qgs} | RADann | RADgs | logMAP | logPPTgs | logMIann |
|-------------------|---------|-----------------|-----------------|-----------------|-------------------|----------|----------|----------|-----------------|-------------------|----------|----------|---------|----------|----------|
| MAT | | | | | | | | | | | | | | | |
| T _{CM} | 0.96*** | | | | | | | | | | | | | | |
| T _{WM} | 0.86*** | 0.70*** | | | | | | | | | | | | | |
| T _{gs} | 0.93*** | 0.87*** | 0.88*** | | | | | | | | | | | | |
| T _{CMgs} | 0.85*** | 0.87*** | 0.66*** | 0.93*** | | | | | | | | | | | |
| cvPPT | 0.11** | 0.02ns | 0.25*** | 0.09* | 0.01ns | | | | | | | | | | |
| RHann | 0.11** | 0.23*** | -0.15*** | 0.13*** | 0.31*** | -0.62*** | | | | | | | | | |
| RHgs | 0.16*** | 0.28*** | -0.10* | 0.18*** | 0.35*** | -0.57*** | 0.99*** | | | | | | | | |
| ET _q | 0.83*** | 0.79*** | 0.72*** | 0.78*** | 0.73*** | 0.37*** | -0.20*** | -0.13*** | | | | | | | |
| ET _{qgs} | 0.84*** | 0.81*** | 0.69*** | 0.77*** | 0.71*** | 0.06ns | -0.06ns | -0.03ns | 0.89*** | | | | | | |
| RADann | 0.68*** | 0.61*** | 0.67*** | 0.60*** | 0.49*** | 0.53*** | -0.47*** | -0.41*** | 0.91*** | 0.77*** | | | | | |
| RADgs | 0.75*** | 0.71*** | 0.64*** | 0.61*** | 0.49*** | 0.11** | -0.24*** | -0.21*** | 0.78*** | 0.92*** | 0.80*** | | | | |
| logMAP | 0.34*** | 0.44*** | 0.05ns | 0.29*** | 0.40*** | -0.59*** | 0.68*** | 0.69*** | 0.11** | 0.25*** | -0.12** | 0.11** | | | |
| logPPTgs | 0.58*** | 0.65*** | 0.32*** | 0.49*** | 0.51*** | -0.47*** | 0.56*** | 0.59*** | 0.32*** | 0.48*** | 0.11** | 0.39*** | 0.87*** | | |
| logMIann | -0.03ns | 0.09* | -0.27*** | -0.04ns | 0.10** | -0.71*** | 0.74*** | 0.73*** | -0.31*** | -0.13*** | -0.51*** | -0.24*** | 0.91*** | 0.68*** | |
| logMIgs | 0.19*** | 0.29*** | -0.05 | 0.15*** | 0.25*** | -0.59*** | 0.73*** | 0.74*** | -0.13*** | 0.01ns | -0.33*** | -0.09* | 0.87*** | 0.86*** | 0.88*** |

Table S1. Pearson correlations among climate variables. The statistical significance is indicated as: * $P < 0.001$; ** $0.001 < P < 0.01$; * $0.01 < P < 0.05$; ns $P > 0.05$.**

Abbreviations: MAT: mean annual temperature (°C); T_{CM}: mean temperature of coldest month (°C), T_{WM}: mean temperature of warmest month (°C); T_{gs}: mean temperature during growing season (°C); T_{CMgs}: mean temperature of coldest month during growing season (°C); cvPPT: coefficient of variation of monthly precipitation (mm); RHann: mean annual daytime relative humidity (%); RHgs: mean daytime relative humidity during growth season (%); ET_q: sum annual equilibrium evapotranspiration (mm); ET_{qgs}: sum growing season equilibrium evapotranspiration (mm); RADann: mean daily irradiance, annual (W.m⁻²); RADgs: mean daily irradiance, growing season (W.m⁻²); logMAP: mean annual sum precipitation, log-transformed (mm); logPPTgs: mean growing season sum precipitation, log-transformed (mm); logMIann: annual equilibrium moisture index, log-transformed (mm.mm⁻¹); logMIgs: growing season equilibrium moisture index, log-transformed (mm.mm⁻¹).

| Climate | r ² | slope | s.e. (slope) | intercept | s.e. (inter) | P | Q05 slope | Q05 inter | Q95 slope | Q95 inter |
|----------------------|----------------|--------|-----------------|-----------|-----------------|----------|--------------|--------------|--------------|--------------|
| MAT | 0.15 | 0.041 | 0.003 | 0.216 | 0.051 | < 0.0001 | 0.079 | -2.171 | 0.028 | 1.535 |
| T _{CM} | 0.16 | 0.029 | 0.002 | 0.582 | 0.03 | < 0.0001 | 0.091 | -1.779 | 0.017 | 1.826 |
| T _{WM} | 0.07 | 0.044 | 0.004 | -0.051 | 0.096 | < 0.0001 | 0.02 | -1.263 | 0.044 | 1.05 |
| T _{gs} | 0.21 | 0.065 | 0.003 | -0.276 | 0.062 | < 0.0001 | 0.115 | -2.813 | 0.044 | 1.164 |
| T _{CMgs} | 0.24 | 0.054 | 0.002 | 0.163 | 0.037 | < 0.0001 | 0.115 | -2.126 | 0.028 | 1.622 |
| logMAP | 0.22 | 1.015 | 0.054 | -2.176 | 0.166 | < 0.0001 | 0.859 | -3.36 | 1.01 | -1.175 |
| cvPPT | 0.08 | -0.006 | 0.001 | 1.365 | 0.055 | < 0.0001 | -0.008 | -0.205 | -0.007 | 2.533 |
| logPPT _{gs} | 0.19 | 0.871 | 0.05 | -1.679 | 0.153 | < 0.0001 | 0.966 | -3.636 | 0.716 | -0.188 |
| logMI _{ann} | 0.12 | 0.698 | 0.059 | 1.003 | 0.021 | < 0.0001 | 0.434 | -0.739 | 0.972 | 2.061 |
| logMI _{gs} | 0.13 | 0.831 | 0.065 | 1.037 | 0.021 | < 0.0001 | 0.516 | -0.708 | 0.919 | 2.1 |
| RAD _{ann} | 0.002 | 0.002 | 0.001 | 0.541 | 0.137 | 0.002 | -1.91E-18 | -0.796 | -1.21E-03 | 2.386 |
| RAD _{gs} | 0.01 | 0.003 | 0.001 | 0.436 | 0.1 | < 0.0001 | -0.796 | -0.796 | 1.888 | 1.888 |
| RH _{ann} | 0.16 | 0.026 | 0.002 | -0.868 | 0.12 | < 0.0001 | 0.021 | -2.198 | 0.022 | 0.44 |
| RH _{gs} | 0.17 | 0.027 | 0.002 | -0.973 | 0.118 | < 0.0001 | 0.022 | 0.039 | 0.023 | 0.081 |
| ET _q | 0.07 | 0.001 | 0.0001 | 0.078 | 0.082 | < 0.0001 | 4.32E-04 | -1.428 | 3.89E-04 | 1.521 |
| ET _{qgs} | 0.09 | 0.001 | 0.0001 | 0.084 | 0.071 | < 0.0001 | 4.05E-04 | -1.371 | 3.99E-04 | 1.517 |

Table S2. Bivariate relationships between log(leaf size, cm²) and individual climate variables.

The r², slope, intercept and P-values refer to linear mixed models in which site and species were treated as random effects; for all relationships sample n = 13461. Q05 and Q95 refer to 5th and 95th linear quantile regressions fitted to the same dataset, as illustrated with dashed lines in Figure 2. Climate abbreviations and units follow those in Table S1.

Table S3. Bivariate relationships between log(leaf size, cm²) and individual climate variables, for species grouped by major growth habit (woody / non-woody) and, for woody species, by phenology (evergreen/deciduous).

The r^2 , slope, intercept and P -values were derived from linear mixed models in which site and species were treated as random effects. Climate abbreviations and units follow Table S1.

| Group | Climate | n | r^2 | slope | s.e. (slope) | intercept | s.e. (inter) | P |
|------------------|----------|-------|-------|--------|-----------------|-----------|-----------------|----------|
| Non-woody | MAT | 2605 | 0.01 | 0.018 | 0.004 | 0.311 | 0.068 | < 0.0001 |
| Woody | MAT | 10856 | 0.15 | 0.043 | 0.003 | 0.207 | 0.054 | < 0.0001 |
| Woody, deciduous | MAT | 1726 | 0.02 | 0.011 | 0.003 | 0.984 | 0.049 | < 0.0001 |
| Woody, evergreen | MAT | 7902 | 0.25 | 0.064 | 0.003 | -0.278 | 0.063 | < 0.0001 |
| Non-woody | TCM | 2605 | 0.008 | 0.014 | 0.003 | 0.473 | 0.039 | < 0.0001 |
| Woody | TCM | 10856 | 0.16 | 0.030 | 0.002 | 0.591 | 0.032 | < 0.0001 |
| Woody, deciduous | TCM | 1726 | 0.01 | 0.007 | 0.002 | 1.104 | 0.030 | < 0.0001 |
| Woody, evergreen | TCM | 7902 | 0.30 | 0.049 | 0.002 | 0.230 | 0.036 | < 0.0001 |
| Non-woody | TCMgs | 2605 | 0.08 | 0.041 | 0.004 | 0.132 | 0.056 | < 0.0001 |
| Woody | TCMgs | 10856 | 0.23 | 0.054 | 0.002 | 0.175 | 0.039 | < 0.0001 |
| Woody, deciduous | TCMgs | 1726 | 0.01 | 0.019 | 0.003 | 0.912 | 0.048 | < 0.0001 |
| Woody, evergreen | TCMgs | 7902 | 0.34 | 0.067 | 0.002 | -0.110 | 0.043 | < 0.0001 |
| Non-woody | Tgs | 2605 | 0.05 | 0.039 | 0.005 | -0.063 | 0.091 | < 0.0001 |
| Woody | Tgs | 10856 | 0.20 | 0.066 | 0.003 | -0.285 | 0.066 | < 0.0001 |
| Woody, deciduous | Tgs | 1726 | 0.04 | 0.024 | 0.004 | 0.716 | 0.079 | < 0.0001 |
| Woody, evergreen | Tgs | 7902 | 0.27 | 0.081 | 0.004 | -0.656 | 0.074 | < 0.0001 |
| Non-woody | TWM | 2605 | 0.009 | 0.017 | 0.005 | 0.215 | 0.114 | 0.001 |
| Woody | TWM | 10856 | 0.07 | 0.045 | 0.004 | -0.049 | 0.103 | < 0.0001 |
| Woody, deciduous | TWM | 1726 | 0.03 | 0.014 | 0.004 | 0.846 | 0.097 | 0.001 |
| Woody, evergreen | TWM | 7902 | 0.09 | 0.057 | 0.005 | -0.412 | 0.119 | < 0.0001 |
| Non-woody | logMAP | 2605 | 0.04 | 0.570 | 0.073 | -1.112 | 0.220 | < 0.0001 |
| Woody | logMAP | 10856 | 0.24 | 1.075 | 0.052 | -2.322 | 0.161 | < 0.0001 |
| Woody, deciduous | logMAP | 1726 | 0.10 | 0.512 | 0.060 | -0.386 | 0.185 | < 0.0001 |
| Woody, evergreen | logMAP | 7902 | 0.29 | 1.237 | 0.056 | -2.908 | 0.177 | < 0.0001 |
| Non-woody | cvPPT | 2605 | 0.02 | -0.003 | 0.001 | 0.820 | 0.079 | 0.002 |
| Woody | cvPPT | 10856 | 0.09 | -0.006 | 0.001 | 1.441 | 0.055 | < 0.0001 |
| Woody, deciduous | cvPPT | 1726 | 0.05 | -0.004 | 0.001 | 1.434 | 0.049 | < 0.0001 |
| Woody, evergreen | cvPPT | 7902 | 0.12 | -0.008 | 0.001 | 1.472 | 0.065 | < 0.0001 |
| Non-woody | logPPTgs | 2605 | 0.03 | 0.406 | 0.068 | -0.595 | 0.198 | < 0.0001 |
| Woody | logPPTgs | 10856 | 0.22 | 0.940 | 0.049 | -1.851 | 0.151 | < 0.0001 |
| Woody, deciduous | logPPTgs | 1726 | 0.09 | 0.413 | 0.052 | -0.043 | 0.156 | < 0.0001 |
| Woody, evergreen | logPPTgs | 7902 | 0.29 | 1.197 | 0.054 | -2.728 | 0.168 | < 0.0001 |
| Non-woody | logMIann | 2605 | 0.02 | 0.372 | 0.068 | 0.632 | 0.031 | < 0.0001 |
| Woody | logMIann | 10856 | 0.15 | 0.777 | 0.058 | 1.053 | 0.021 | < 0.0001 |
| Woody, deciduous | logMIann | 1726 | 0.06 | 0.408 | 0.059 | 1.207 | 0.025 | < 0.0001 |

| | | | | | | | | |
|------------------|-------------------|-------|---------|---------|-------|--------|-------|----------|
| Woody, evergreen | logMIann | 7902 | 0.17 | 0.843 | 0.066 | 0.981 | 0.024 | < 0.0001 |
| Non-woody | logMIgs | 2605 | 0.02 | 0.395 | 0.077 | 0.651 | 0.032 | < 0.0001 |
| Woody | logMIgs | 10856 | 0.15 | 0.916 | 0.065 | 1.087 | 0.021 | < 0.0001 |
| Woody, deciduous | logMIgs | 1726 | 0.06 | 0.458 | 0.067 | 1.233 | 0.027 | < 0.0001 |
| Woody, evergreen | logMIgs | 7902 | 0.18 | 1.037 | 0.073 | 1.018 | 0.024 | < 0.0001 |
| Non-woody | RAD | 2605 | < 0.001 | 0.0005 | 0.001 | 0.499 | 0.147 | 0.548 |
| Woody | RAD | 10856 | < 0.001 | 0.002 | 0.001 | 0.545 | 0.148 | 0.003 |
| Woody, deciduous | RAD | 1726 | < 0.001 | -0.0001 | 0.001 | 1.187 | 0.105 | 0.863 |
| Woody, evergreen | RAD | 7902 | < 0.001 | 0.004 | 0.001 | 0.067 | 0.180 | < 0.0001 |
| Non-woody | RADgs | 2605 | < 0.001 | 0.0004 | 0.001 | 0.509 | 0.108 | 0.453 |
| Woody | RADgs | 10856 | 0.01 | 0.003 | 0.001 | 0.417 | 0.107 | < 0.0001 |
| Woody, deciduous | RADgs | 1726 | 0.01 | 0.001 | 0.000 | 1.031 | 0.076 | 0.059 |
| Woody, evergreen | RADgs | 7902 | 0.01 | 0.006 | 0.001 | -0.153 | 0.133 | < 0.0001 |
| Non-woody | RHann | 2605 | 0.03 | 0.013 | 0.002 | -0.268 | 0.146 | < 0.0001 |
| Woody | RHann | 10856 | 0.18 | 0.028 | 0.002 | -0.966 | 0.117 | < 0.0001 |
| Woody, deciduous | RHann | 1726 | 0.02 | 0.011 | 0.002 | 0.377 | 0.147 | < 0.0001 |
| Woody, evergreen | RHann | 7902 | 0.22 | 0.030 | 0.002 | -1.189 | 0.129 | < 0.0001 |
| Non-woody | RHgs | 2605 | 0.03 | 0.013 | 0.002 | -0.308 | 0.146 | < 0.0001 |
| Woody | RHgs | 10856 | 0.19 | 0.029 | 0.002 | -1.069 | 0.115 | < 0.0001 |
| Woody, deciduous | RHgs | 1726 | 0.03 | 0.011 | 0.002 | 0.353 | 0.149 | < 0.0001 |
| Woody, evergreen | RHgs | 7902 | 0.23 | 0.032 | 0.002 | -1.300 | 0.127 | < 0.0001 |
| Non-woody | ET _q | 2605 | 0.008 | 0.0003 | 0.000 | 0.220 | 0.097 | < 0.0001 |
| Woody | ET _q | 10856 | 0.07 | 0.001 | 0.000 | 0.040 | 0.090 | < 0.0001 |
| Woody, deciduous | ET _q | 1726 | 0.009 | 0.0001 | 0.000 | 1.027 | 0.074 | 0.048 |
| Woody, evergreen | ET _q | 7902 | 0.10 | 0.001 | 0.000 | -0.494 | 0.106 | < 0.0001 |
| Non-woody | ET _{qgs} | 2605 | 0.01 | 0.0002 | 0.000 | 0.272 | 0.085 | < 0.0001 |
| Woody | ET _{qgs} | 10856 | 0.09 | 0.001 | 0.000 | 0.037 | 0.077 | < 0.0001 |
| Woody, deciduous | ET _{qgs} | 1726 | 0.03 | 0.0002 | 0.000 | 0.932 | 0.065 | 0.0001 |
| Woody, evergreen | ET _{qgs} | 7902 | 0.13 | 0.001 | 0.000 | -0.501 | 0.090 | < 0.0001 |

Table S4. Bivariate relationships between log(leaf size, cm²) and individual climate variables, for species grouped by growth form.

The r^2 , slope, intercept and P-values were derived from linear mixed models in which site and species were treated as random effects. Climate abbreviations and units follow Table S1.

| Group | Climate | n | r ² | slope | intercept | P | Group | Climate | n | r ² | slope | intercept | P |
|-------|-------------------|------|----------------|----------|-----------|----------|-------|-------------------|------|----------------|--------|-----------|----------|
| Fern | MAT | 312 | 0.08 | 0.057 | -0.774 | < 0.0001 | Shrub | MAT | 2805 | 0.04 | 0.024 | 0.095 | < 0.0001 |
| Fern | T _{CM} | 312 | 0.07 | 0.045 | -0.389 | < 0.0001 | Shrub | T _{CM} | 2805 | 0.05 | 0.018 | 0.310 | < 0.0001 |
| Fern | T _{WM} | 312 | 0.07 | 0.060 | -1.084 | < 0.0001 | Shrub | T _{WM} | 2805 | 0.01 | 0.021 | 0.023 | 0.0001 |
| Fern | T _{gs} | 312 | 0.07 | 0.055 | -0.768 | < 0.0001 | Shrub | T _{gs} | 2805 | 0.10 | 0.056 | -0.490 | < 0.0001 |
| Fern | T _{CMgs} | 312 | 0.05 | 0.039 | -0.365 | 0.001 | Shrub | T _{CMgs} | 2805 | 0.15 | 0.056 | -0.214 | < 0.0001 |
| Fern | RHann | 312 | 0.04 | -0.009 | 0.686 | 0.034 | Shrub | RHann | 2805 | 0.14 | 0.025 | -1.220 | < 0.0001 |
| Fern | RHgs | 312 | 0.03 | -0.007 | 0.540 | 0.095 | Shrub | RHgs | 2805 | 0.14 | 0.026 | -1.247 | < 0.0001 |
| Fern | ET _q | 312 | 0.09 | 0.001 | -0.736 | < 0.0001 | Shrub | ET _q | 2805 | 0.03 | 0.0004 | -0.121 | < 0.0001 |
| Fern | ET _{qgs} | 312 | 0.09 | 0.001 | -0.738 | < 0.0001 | Shrub | ET _{qgs} | 2805 | 0.03 | 0.0004 | -0.064 | < 0.0001 |
| Fern | RAD | 312 | 0.08 | 0.007 | -1.147 | < 0.0001 | Shrub | RAD | 2805 | 0.001 | 0.001 | 0.334 | 0.367 |
| Fern | RADgs | 312 | 0.09 | 0.007 | -1.106 | < 0.0001 | Shrub | RADgs | 2805 | < 0.001 | 0.001 | 0.327 | 0.166 |
| Fern | logMAP | 312 | < 0.001 | 0.159 | -0.512 | 0.067 | Shrub | logMAP | 2805 | 0.15 | 0.825 | -1.975 | < 0.0001 |
| Fern | logPPTgs | 312 | < 0.001 | 0.258 | -0.812 | 0.003 | Shrub | logPPTgs | 2805 | 0.10 | 0.621 | -1.324 | < 0.0001 |
| Fern | cvPPT | 312 | 0.03 | 0.003 | -0.133 | 0.198 | Shrub | cvPPT | 2805 | 0.05 | -0.006 | 0.922 | < 0.0001 |
| Fern | logMIann | 312 | < 0.001 | 0.063 | -0.007 | 0.465 | Shrub | logMIann | 2805 | 0.09 | 0.623 | 0.582 | < 0.0001 |
| Fern | logMIgs | 312 | < 0.001 | 0.154 | -0.016 | 0.092 | Shrub | logMIgs | 2805 | 0.08 | 0.656 | 0.605 | < 0.0001 |
| Grass | MAT | 489 | 0.01 | -0.014 | 0.665 | 0.035 | Tree | MAT | 6559 | 0.12 | 0.032 | 0.678 | < 0.0001 |
| Grass | T _{CM} | 489 | 0.01 | -0.009 | 0.524 | 0.066 | Tree | T _{CM} | 6559 | 0.11 | 0.021 | 0.993 | < 0.0001 |
| Grass | T _{WM} | 489 | 0.006 | -0.019 | 0.873 | 0.028 | Tree | T _{WM} | 6559 | 0.09 | 0.037 | 0.432 | < 0.0001 |
| Grass | T _{gs} | 489 | 0.002 | -0.008 | 0.602 | 0.475 | Tree | T _{gs} | 6559 | 0.15 | 0.043 | 0.443 | < 0.0001 |
| Grass | T _{CMgs} | 489 | < 0.001 | 0.011 | 0.380 | 0.375 | Tree | T _{CMgs} | 6559 | 0.15 | 0.032 | 0.779 | < 0.0001 |
| Grass | RHann | 489 | 0.007 | 0.014 | -0.421 | < 0.0001 | Tree | RHann | 6559 | 0.08 | 0.017 | 0.072 | < 0.0001 |
| Grass | RHgs | 489 | 0.01 | 0.014 | -0.426 | < 0.0001 | Tree | RHgs | 6559 | 0.09 | 0.018 | 0.007 | < 0.0001 |
| Grass | ET _q | 489 | 0.005 | -0.0003 | 0.800 | 0.023 | Tree | ET _q | 6559 | 0.04 | 0.0004 | 0.626 | < 0.0001 |
| Grass | ET _{qgs} | 489 | 0.006 | -0.0002 | 0.772 | 0.013 | Tree | ET _{qgs} | 6559 | 0.06 | 0.0005 | 0.578 | < 0.0001 |
| Grass | RAD | 489 | 0.003 | -0.003 | 1.100 | 0.002 | Tree | RAD | 6559 | < 0.001 | 0.001 | 1.019 | 0.025 |
| Grass | RADgs | 489 | 0.008 | -0.003 | 0.947 | 0.001 | Tree | RADgs | 6559 | 0.01 | 0.003 | 0.791 | < 0.0001 |
| Grass | logMAP | 489 | 0.03 | 0.450 | -0.822 | 0.0001 | Tree | logMAP | 6559 | 0.13 | 0.667 | -0.799 | < 0.0001 |
| Grass | logPPTgs | 489 | 0.01 | 0.192 | -0.064 | 0.056 | Tree | logPPTgs | 6559 | 0.13 | 0.665 | -0.756 | < 0.0001 |
| Grass | cvPPT | 489 | 0.02 | -0.005 | 0.867 | 0.001 | Tree | cvPPT | 6559 | 0.06 | -0.005 | 1.653 | < 0.0001 |
| Grass | logMIann | 489 | 0.02 | 0.392 | 0.548 | < 0.0001 | Tree | logMIann | 6559 | 0.07 | 0.486 | 1.320 | < 0.0001 |
| Grass | logMIgs | 489 | 0.03 | 0.386 | 0.562 | 0.001 | Tree | logMIgs | 6559 | 0.07 | 0.569 | 1.338 | < 0.0001 |
| Herb | MAT | 1363 | < 0.001 | 0.003 | 0.469 | 0.619 | Liana | MAT | 1409 | 0.03 | 0.010 | 1.183 | < 0.0001 |
| Herb | T _{CM} | 1363 | < 0.001 | 0.004 | 0.488 | 0.412 | Liana | T _{CM} | 1409 | 0.03 | 0.008 | 1.249 | < 0.0001 |
| Herb | T _{WM} | 1363 | 0.002 | -0.002 | 0.548 | 0.806 | Liana | T _{WM} | 1409 | 0.02 | 0.009 | 1.182 | 0.001 |
| Herb | T _{gs} | 1363 | < 0.001 | 0.021 | 0.181 | 0.019 | Liana | T _{gs} | 1409 | 0.04 | 0.012 | 1.137 | < 0.0001 |
| Herb | T _{CMgs} | 1363 | < 0.001 | 0.032 | 0.195 | < 0.0001 | Liana | T _{CMgs} | 1409 | 0.04 | 0.010 | 1.223 | < 0.0001 |
| Herb | RHann | 1363 | 0.12 | 0.019 | -0.774 | < 0.0001 | Liana | RHann | 1409 | 0.03 | 0.004 | 1.128 | 0.002 |
| Herb | RHgs | 1363 | 0.12 | 0.020 | -0.791 | < 0.0001 | Liana | RHgs | 1409 | 0.03 | 0.004 | 1.114 | 0.001 |
| Herb | ET _q | 1363 | 0.009 | -0.0001 | 0.592 | 0.523 | Liana | ET _q | 1409 | 0.01 | 0.0001 | 1.209 | 0.005 |
| Herb | ET _{qgs} | 1363 | 0.002 | -0.00001 | 0.527 | 0.872 | Liana | ET _{qgs} | 1409 | 0.02 | 0.0001 | 1.201 | 0.001 |
| Herb | RAD | 1363 | 0.04 | -0.003 | 0.998 | 0.011 | Liana | RAD | 1409 | < 0.001 | 0.001 | 1.290 | 0.306 |

| | | | | | | | | | | | | | |
|------|--------------------|------|---------|--------|--------|----------|-------|----------|------|-------|--------|-------|----------|
| Herb | RADgs | 1363 | 0.02 | -0.001 | 0.746 | 0.073 | Liana | RADgs | 1409 | 0.002 | 0.001 | 1.252 | 0.071 |
| Herb | logMAP | 1363 | 0.09 | 0.646 | -1.366 | < 0.0001 | Liana | logMAP | 1409 | 0.03 | 0.179 | 0.832 | < 0.0001 |
| Herb | logPPTgs | 1363 | 0.04 | 0.376 | -0.551 | < 0.0001 | Liana | logPPTgs | 1409 | 0.03 | 0.171 | 0.862 | 0.0003 |
| Herb | cvPPT | 1363 | 0.10 | -0.007 | 1.044 | < 0.0001 | Liana | cvPPT | 1409 | 0.01 | -0.001 | 1.469 | 0.046 |
| Herb | logMIann | 1363 | 0.10 | 0.539 | 0.612 | < 0.0001 | Liana | logMIann | 1409 | 0.02 | 0.127 | 1.406 | 0.002 |
| Herb | logMIgs | 1363 | 0.08 | 0.538 | 0.634 | < 0.0001 | Liana | logMIgs | 1409 | 0.01 | 0.101 | 1.407 | 0.029 |
| Vine | MAT | 377 | 0.06 | 0.010 | 1.076 | 0.014 | | | | | | | |
| Vine | T _{CM} | 377 | 0.07 | 0.010 | 1.131 | 0.004 | | | | | | | |
| Vine | T _{WM} | 377 | 0.02 | 0.006 | 1.148 | 0.183 | | | | | | | |
| Vine | T _{gs} | 377 | 0.06 | 0.010 | 1.082 | 0.018 | | | | | | | |
| Vine | T _{CMgs} | 377 | 0.08 | 0.011 | 1.112 | 0.003 | | | | | | | |
| Vine | RHann | 377 | < 0.001 | 0.003 | 1.080 | 0.182 | | | | | | | |
| Vine | RHgs | 377 | < 0.001 | 0.003 | 1.082 | 0.185 | | | | | | | |
| Vine | ET _a | 377 | 0.08 | 0.0002 | 0.930 | 0.003 | | | | | | | |
| Vine | ET _a gs | 377 | 0.08 | 0.0002 | 0.967 | 0.004 | | | | | | | |
| Vine | RAD | 377 | 0.04 | 0.002 | 0.866 | 0.027 | | | | | | | |
| Vine | RADgs | 377 | 0.04 | 0.002 | 0.975 | 0.042 | | | | | | | |
| Vine | logMAP | 377 | 0.005 | 0.101 | 0.970 | 0.163 | | | | | | | |
| Vine | logPPTgs | 377 | 0.003 | 0.074 | 1.056 | 0.366 | | | | | | | |
| Vine | cvPPT | 377 | < 0.001 | -0.001 | 1.341 | 0.446 | | | | | | | |
| Vine | logMIann | 377 | < 0.001 | 0.029 | 1.289 | 0.680 | | | | | | | |
| Vine | logMIgs | 377 | 0.002 | -0.019 | 1.287 | 0.813 | | | | | | | |

References and Notes

1. H. G. Jones, *Plants and Microclimate: A Quantitative Approach to Environmental Plant Physiology* (Cambridge Univ. Press, ed. 3, 2014).
2. D. M. Gates, Energy, plants and ecology. *Ecology* **46**, 1–13 (1965). [doi:10.2307/1935252](https://doi.org/10.2307/1935252)
3. W. Larcher, *Physiological Plant Ecology. Ecophysiology and Stress Ecology of Functional Groups* (Springer-Verlag, ed. 4, 2003).
4. G. S. Campbell, J. M. Norman, *An Introduction to Environmental Biophysics* (Springer, ed. 2, 1998).
5. S. T. Michaletz, M. D. Weiser, N. G. McDowell, J. Zhou, M. Kaspari, B. R. Helliker, B. J. Enquist, The energetic and carbon economic origins of leaf thermoregulation. *Nat. Plants* **2**, 16129 (2016). [doi:10.1038/nplants.2016.129](https://doi.org/10.1038/nplants.2016.129) [Medline](#)
6. T. J. Givnish, Comparative studies of leaf form: Assessing the relative roles of selective pressures and phylogenetic constraints. *New Phytol.* **106** (suppl.), 131–160 (1987). [doi:10.1111/j.1469-8137.1987.tb04687.x](https://doi.org/10.1111/j.1469-8137.1987.tb04687.x)
7. C. Körner, M. Neumayer, S. P. Menendez-Riedl, A. Smeets-Scheel, Functional morphology of mountain plants. *Flora* **182**, 353–383 (1989). [doi:10.1016/S0367-2530\(17\)30426-7](https://doi.org/10.1016/S0367-2530(17)30426-7)
8. S. Díaz, J. Kattge, J. H. C. Cornelissen, I. J. Wright, S. Lavorel, S. Dray, B. Reu, M. Kleyer, C. Wirth, I. C. Prentice, E. Garnier, G. Bönsch, M. Westoby, H. Poorter, P. B. Reich, A. T. Moles, J. Dickie, A. N. Gillison, A. E. Zanne, J. Chave, S. J. Wright, S. N. Sheremet'ev, H. Jactel, C. Baraloto, B. Cerabolini, S. Pierce, B. Shipley, D. Kirkup, F. Casanoves, J. S. Joswig, A. Günther, V. Falczuk, N. Rüger, M. D. Mahecha, L. D. Gorné, The global spectrum of plant form and function. *Nature* **529**, 167–171 (2016). [doi:10.1038/nature16489](https://doi.org/10.1038/nature16489) [Medline](#)
9. D. M. Gates, Transpiration and leaf temperature. *Annu. Rev. Plant Physiol.* **19**, 211–238 (1968). [doi:10.1146/annurev.pp.19.060168.001235](https://doi.org/10.1146/annurev.pp.19.060168.001235)
10. A. Leigh, S. Sevanto, J. D. Close, A. B. Nicotra, The influence of leaf size and shape on leaf thermal dynamics: Does theory hold up under natural conditions? *Plant Cell Environ.* **40**, 237–248 (2017). [doi:10.1111/pce.12857](https://doi.org/10.1111/pce.12857) [Medline](#)
11. D. F. Parkhurst, O. L. Loucks, Optimal leaf size in relation to environment. *J. Ecol.* **60**, 505–537 (1972). [doi:10.2307/2258359](https://doi.org/10.2307/2258359)
12. T. J. Givnish, G. J. Vermeij, Sizes and shapes of liane leaves. *Am. Nat.* **110**, 743–778 (1976). [doi:10.1086/283101](https://doi.org/10.1086/283101)
13. T. J. Givnish, in *Physiological Ecology of Plants of the Wet Tropics*, E. Medina, H. A. Mooney, C. Vázquez-Yánes, Eds. (Dr W Junk Publishers, 1984), pp. 51–84.
14. S. E. Taylor, in *Perspectives of Biophysical Ecology*, D. M. Gates, R. B. Schmerl, Eds. (Springer-Verlag, 1975), pp. 73–86.
15. B. F. Jacobs, Estimation of rainfall variables from leaf characters in tropical Africa. *Palaeogeogr. Palaeoclimatol. Palaeoecol.* **145**, 231–250 (1999). [doi:10.1016/S0031-0182\(98\)00102-3](https://doi.org/10.1016/S0031-0182(98)00102-3)

16. P. Wilf, S. L. Wing, D. R. Greenwood, C. L. Greenwood, Using fossil leaves as paleoprecipitation indicators: An Eocene example. *Geology* **26**, 203–206 (1998). [doi:10.1130/0091-7613\(1998\)026<0203:UFLAPI>2.3.CO;2](https://doi.org/10.1130/0091-7613(1998)026<0203:UFLAPI>2.3.CO;2)
17. C. R. Fonseca, J. M. Overton, B. Collins, M. Westoby, Shifts in trait combinations along rainfall and phosphorus gradients. *J. Ecol.* **88**, 964–977 (2000). [doi:10.1046/j.1365-2745.2000.00506.x](https://doi.org/10.1046/j.1365-2745.2000.00506.x)
18. A. T. Moles, S. E. Perkins, S. W. Laffan, H. Flores-Moreno, M. Awasthy, M. L. Tindall, L. Sack, A. Pitman, J. Kattge, L. W. Aarssen, M. Anand, M. Bahn, B. Blonder, J. Cavender-Bares, J. H. C. Cornelissen, W. K. Cornwell, S. Díaz, J. B. Dickie, G. T. Freschet, J. G. Griffiths, A. G. Gutierrez, F. A. Hemmings, T. Hickler, T. D. Hitchcock, M. Keighery, M. Kleyer, H. Kurokawa, M. R. Leishman, K. Liu, Ü. Niinemets, V. Onipchenko, Y. Onoda, J. Penuelas, V. D. Pillar, P. B. Reich, S. Shiodera, A. Siefert, E. E. Sosinski Jr., N. A. Soudzilovskaia, E. K. Swaine, N. G. Swenson, P. M. van Bodegom, L. Warman, E. Weiher, I. J. Wright, H. Zhang, M. Zobel, S. P. Bonser, Which is a better predictor of plant traits: Temperature or precipitation? *J. Veg. Sci.* **25**, 1167–1180 (2014). [doi:10.1111/jvs.12190](https://doi.org/10.1111/jvs.12190)
19. D. J. Peppe, D. L. Royer, B. Cariglino, S. Y. Oliver, S. Newman, E. Leight, G. Enikolopov, M. Fernandez-Burgos, F. Herrera, J. M. Adams, E. Correa, E. D. Currano, J. M. Erickson, L. F. Hinojosa, J. W. Hoganson, A. Iglesias, C. A. Jaramillo, K. R. Johnson, G. J. Jordan, N. J. B. Kraft, E. C. Lovelock, C. H. Lusk, U. Niinemets, J. Peñuelas, G. Rapon, S. L. Wing, I. J. Wright, Sensitivity of leaf size and shape to climate: Global patterns and paleoclimatic applications. *New Phytol.* **190**, 724–739 (2011). [doi:10.1111/j.1469-8137.2010.03615.x](https://doi.org/10.1111/j.1469-8137.2010.03615.x) [Medline](#)
20. D. Ackerly, C. Knight, S. Weiss, K. Barton, K. Starmer, Leaf size, specific leaf area and microhabitat distribution of chaparral woody plants: Contrasting patterns in species level and community level analyses. *Oecologia* **130**, 449–457 (2002). [doi:10.1007/s004420100805](https://doi.org/10.1007/s004420100805) [Medline](#)
21. D. R. Greenwood, Taphonomic constraints on foliar physiognomic interpretations of Late Cretaceous and Tertiary paleoclimates. *Rev. Palaeobot. Palynol.* **71**, 149–190 (1992). [doi:10.1016/0034-6667\(92\)90161-9](https://doi.org/10.1016/0034-6667(92)90161-9)
22. S. R. P. Halloy, A. F. Mark, Comparative leaf morphology spectra of plant communities in New Zealand, the Andes and the European Alps. *J. R. Soc. N. Z.* **26**, 41–78 (1996). [doi:10.1080/03014223.1996.9517504](https://doi.org/10.1080/03014223.1996.9517504)
23. R. Leuning, Leaf temperatures during radiation frost Part II. A steady state theory. *Agric. Meteorol.* **42**, 135–155 (1988). [doi:10.1016/0168-1923\(88\)90073-1](https://doi.org/10.1016/0168-1923(88)90073-1)
24. D. N. Jordan, W. K. Smith, Energy balance analysis of night-time leaf temperatures and frost formation in a subalpine environment. *Agric. Meteorol.* **71**, 359–372 (1994). [doi:10.1016/0168-1923\(94\)90020-5](https://doi.org/10.1016/0168-1923(94)90020-5)
25. A. F. W. Schimper, *Plant Geography Upon a Physiological Basis* (Clarendon Press, 1903).
26. E. Warming, *Oecology of Plants* (Clarendon Press, 1909).

27. E. M. Curtis, C. A. Knight, K. Petrou, A. Leigh, A comparative analysis of photosynthetic recovery from thermal stress: A desert plant case study. *Oecologia* **175**, 1051–1061 (2014). [doi:10.1007/s00442-014-2988-5](https://doi.org/10.1007/s00442-014-2988-5) [Medline](#)
28. Z. H. Hu, Y. N. Xu, Y. D. Gong, T. Y. Kuang, Effects of heat treatment on the protein secondary structure and pigment microenvironment in photosystem 1 complex. *Photosynthetica* **43**, 529–534 (2005). [doi:10.1007/s11099-005-0085-z](https://doi.org/10.1007/s11099-005-0085-z)
29. Y. Vitasse, A. Lenz, G. Hoch, C. Körner, Earlier leaf-out rather than difference in freezing resistance puts juvenile trees at greater risk of damage than adult trees. *J. Ecol.* **102**, 981–988 (2014). [doi:10.1111/1365-2745.12251](https://doi.org/10.1111/1365-2745.12251)
30. K. H. Jensen, M. A. Zwieniecki, Physical limits to leaf size in tall trees. *Phys. Rev. Lett.* **110**, 018104 (2013). [doi:10.1103/PhysRevLett.110.018104](https://doi.org/10.1103/PhysRevLett.110.018104) [Medline](#)
31. M. R. Raupach, Combination theory and equilibrium evaporation. *Q. J. R. Meteorol. Soc.* **127**, 1149–1181 (2001). [doi:10.1002/qj.49712757402](https://doi.org/10.1002/qj.49712757402)
32. C. Huntingford, J. L. Monteith, The behaviour of a mixed-layer model of the convective boundary layer coupled to a big leaf model of surface energy partitioning. *Boundary-Layer Meteorol.* **88**, 87–101 (1998). [doi:10.1023/A:1001110819090](https://doi.org/10.1023/A:1001110819090)
33. N. Chiariello, in *Physiological Ecology of Plants of the Wet Tropics*, E. Medina, H. A. Mooney, C. Vázquez-Yanes, Eds. (Dr W Junk Publishers, 1984), pp. 85–98.
34. D. D. Ackerly, Functional strategies of chaparral shrubs in relation to seasonal water deficit and disturbance. *Ecol. Monogr.* **74**, 25–44 (2004). [doi:10.1890/03-4022](https://doi.org/10.1890/03-4022)
35. I. J. Wright, D. S. Falster, M. Pickup, M. Westoby, Cross-species patterns in the coordination between leaf and stem traits, and their implications for plant hydraulics. *Physiol. Plant.* **127**, 445–456 (2006). [doi:10.1111/j.1399-3054.2006.00699.x](https://doi.org/10.1111/j.1399-3054.2006.00699.x)
36. U. Niinemets, A. Portsmouth, D. Tena, M. Tobias, S. Matesanz, F. Valladares, Do we underestimate the importance of leaf size in plant economics? Disproportional scaling of support costs within the spectrum of leaf physiognomy. *Ann. Bot.* **100**, 283–303 (2007). [doi:10.1093/aob/mcm107](https://doi.org/10.1093/aob/mcm107) [Medline](#)
37. M. Pickup, M. Westoby, A. Basden, Dry mass costs of deploying leaf area in relation to leaf size. *Funct. Ecol.* **19**, 88–97 (2005). [doi:10.1111/j.0269-8463.2005.00927.x](https://doi.org/10.1111/j.0269-8463.2005.00927.x)
38. W. K. Smith, Temperatures of desert plants: Another perspective on the adaptability of leaf size. *Science* **201**, 614–616 (1978). [doi:10.1126/science.201.4356.614](https://doi.org/10.1126/science.201.4356.614) [Medline](#)
39. N. Dong, I. C. Prentice, S. P. Harrison, Q. H. Song, Y. P. Zhang, Biophysical homeostasis of leaf temperature: A neglected process for vegetation and land-surface modelling. *Glob. Ecol. Biogeogr.* **26**, 998–1007 (2017). [doi:10.1111/geb.12614](https://doi.org/10.1111/geb.12614)
40. L. Sack, C. Scoffoni, A. D. McKown, K. Frole, M. Rawls, J. C. Havran, H. Tran, T. Tran, Developmentally based scaling of leaf venation architecture explains global ecological patterns. *Nat. Commun.* **3**, 837 (2012). [doi:10.1038/ncomms1835](https://doi.org/10.1038/ncomms1835) [Medline](#)
41. A. T. Moles, M. Westoby, Do small leaves expand faster than large leaves, and do shorter expansion times reduce herbivore damage? *Oikos* **90**, 517–524 (2000). [doi:10.1034/j.1600-0706.2000.900310.x](https://doi.org/10.1034/j.1600-0706.2000.900310.x)

42. I. W. Bailey, E. W. Sinnott, A botanical index of Cretaceous and Tertiary climate. *Science* **41**, 831–834 (1915). [doi:10.1126/science.41.1066.831](https://doi.org/10.1126/science.41.1066.831) [Medline](#)
43. I. J. Wright, P. B. Reich, M. Westoby, D. D. Ackerly, Z. Baruch, F. Bongers, J. Cavender-Bares, T. Chapin, J. H. C. Cornelissen, M. Diemer, J. Flexas, E. Garnier, P. K. Groom, J. Gulias, K. Hikosaka, B. B. Lamont, T. Lee, W. Lee, C. Lusk, J. J. Midgley, M.-L. Navas, U. Niinemets, J. Oleksyn, N. Osada, H. Poorter, P. Poot, L. Prior, V. I. Pyankov, C. Roumet, S. C. Thomas, M. G. Tjoelker, E. J. Veneklaas, R. Villar, The worldwide leaf economics spectrum. *Nature* **428**, 821–827 (2004). [doi:10.1038/nature02403](https://doi.org/10.1038/nature02403) [Medline](#)
44. I. J. Wright, D. D. Ackerly, F. Bongers, K. E. Harms, G. Ibarra-Manriquez, M. Martinez-Ramos, S. J. Mazer, H. C. Muller-Landau, H. Paz, N. C. A. Pitman, L. Poorter, M. R. Silman, C. F. Vriesendorp, C. O. Webb, M. Westoby, S. J. Wright, Relationships among ecologically important dimensions of plant trait variation in seven neotropical forests. *Ann. Bot.* **99**, 1003–1015 (2007). [doi:10.1093/aob/mcl066](https://doi.org/10.1093/aob/mcl066) [Medline](#)
45. R. V. Gallagher, M. R. Leishman, A global analysis of trait variation and evolution in climbing plants. *J. Biogeogr.* **39**, 1757–1771 (2012). [doi:10.1111/j.1365-2699.2012.02773.x](https://doi.org/10.1111/j.1365-2699.2012.02773.x)
46. C. Raunkjær, in *Life Forms of Plants and Statistical Plant Geography* (Clarendon Press, 1934), chap. 10, pp. 369–378.
47. N. Pérez-Harguindeguy, S. Díaz, E. Garnier, S. Lavorel, H. Poorter, P. Jaureguiberry, M. S. Bret-Harte, W. K. Cornwell, J. M. Craine, D. E. Gurvich, C. Urcelay, E. J. Veneklaas, P. B. Reich, L. Poorter, I. J. Wright, P. Ray, L. Enrico, J. G. Pausas, A. C. de Vos, N. Buchmann, G. Funes, F. Quétier, J. G. Hodgson, K. Thompson, H. D. Morgan, H. ter Steege, L. Sack, B. Blonder, P. Poschlod, M. V. Vaieretti, G. Conti, A. C. Staver, S. Aquino, J. H. C. Cornelissen, New handbook for standardised measurement of plant functional traits worldwide. *Aust. J. Bot.* **61**, 167–234 (2013). [doi:10.1071/BT12225](https://doi.org/10.1071/BT12225)
48. J. Kattge, S. Díaz, S. Lavorel, I. C. Prentice, P. Leadley, G. Bönsch, E. Garnier, M. Westoby, P. B. Reich, I. J. Wright, J. H. C. Cornelissen, C. Violle, S. P. Harrison, P. M. Van BODEGOM, M. Reichstein, B. J. Enquist, N. A. Soudzilovskaia, D. D. Ackerly, M. Anand, O. Atkin, M. Bahn, T. R. Baker, D. Baldocchi, R. Bekker, C. C. Blanco, B. Blonder, W. J. Bond, R. Bradstock, D. E. Bunker, F. Casanoves, J. Cavender-Bares, J. Q. Chambers, F. S. Chapin III, J. Chave, D. Coomes, W. K. Cornwell, J. M. Craine, B. H. Dobrin, L. Duarte, W. Durka, J. Elser, G. Esser, M. Estiarte, W. F. Fagan, J. Fang, F. Fernández-Méndez, A. Fidelis, B. Finegan, O. Flores, H. Ford, D. Frank, G. T. Freschet, N. M. Fyllas, R. V. Gallagher, W. A. Green, A. G. Gutierrez, T. Hickler, S. I. Higgins, J. G. Hodgson, A. Jalili, S. Jansen, C. A. Joly, A. J. Kerkhoff, D. Kirkup, K. Kitajima, M. Kleyer, S. Klotz, J. M. H. Knops, K. Kramer, I. Kühn, H. Kurokawa, D. Laughlin, T. D. Lee, M. Leishman, F. Lens, T. Lenz, S. L. Lewis, J. Lloyd, J. Llusià, F. Louault, S. Ma, M. D. Mahecha, P. Manning, T. Massad, B. E. Medlyn, J. Messier, A. T. Moles, S. C. Müller, K. Nadrowski, S. Naeem, Ü. Niinemets, S. Nöllert, A. Nüske, R. Ogaya, J. Oleksyn, V. G. Onipchenko, Y. Onoda, J. Ordoñez, G. Overbeck, W. A. Ozinga, S. Patiño, S. Paula, J. G. Pausas, J. Peñuelas, O. L. Phillips, V. Pillar, H. Poorter, L. Poorter, P. Poschlod, A. Prinzing, R. Proulx, A. Rammig, S. Reinsch, B. Reu, L. Sack, B. Salgado-Negret, J. Sardans, S. Shiodera, B. Shipley, A. Siefert, E. Sosinski, J.-F. Soussana, E. Swaine, N. Swenson, K. Thompson, P. Thornton, M. Waldram, E. Weiher,

- M. White, S. White, S. J. Wright, B. Yguel, S. Zaehle, A. E. Zanne, C. Wirth, TRY—A global database of plant traits. *Glob. Change Biol.* **17**, 2905–2935 (2011). [doi:10.1111/j.1365-2486.2011.02451.x](https://doi.org/10.1111/j.1365-2486.2011.02451.x)
49. E. Garnier, U. Stahl, M.-A. Laporte, J. Kattge, I. Mougnot, I. Kühn, B. Laporte, B. Amiaud, F. S. Ahrestani, G. Bönisch, D. E. Bunker, J. H. C. Cornelissen, S. Díaz, B. J. Enquist, S. Gachet, P. Jaureguiberry, M. Kleyer, S. Lavorel, L. Maicher, N. Pérez-Harguindeguy, H. Poorter, M. Schildhauer, B. Shipley, C. Violle, E. Weiher, C. Wirth, I. J. Wright, S. Klotz, Towards a thesaurus of plant characteristics: An ecological contribution. *J. Ecol.* **105**, 298–309 (2017). [doi:10.1111/1365-2745.12698](https://doi.org/10.1111/1365-2745.12698)
50. G. E. Dolph, The effect of different calculational techniques on the estimation of leaf area and the construction of leaf size distributions. *Bull. Torrey Bot. Club* **104**, 264–269 (1977). [doi:10.2307/2484308](https://doi.org/10.2307/2484308)
51. S. A. Cain, G. M. de Oliveira Castro, J. Murça Pires, N. T. da Silva, Application of some phytosociological techniques to Brazilian rain forest. *Am. J. Bot.* **43**, 911–941 (1956). [doi:10.2307/2439008](https://doi.org/10.2307/2439008)
52. D. J. Peppe, D. L. Royer, P. Wilf, E. A. Kowalski, Quantification of large uncertainties in fossil leaf paleoaltimetry. *Tectonics* **29**, TC3015 (2010). [doi:10.1029/2009TC002549](https://doi.org/10.1029/2009TC002549)
53. A. R. Smith, K. M. Pryer, E. Schuettpelz, P. Korall, H. Schneider, P. G. Wolf, A classification for extant ferns. *Taxon* **55**, 705–731 (2006). [doi:10.2307/25065646](https://doi.org/10.2307/25065646)
54. D. J. Mabberley, *Mabberley's Plant-Book: A Portable Dictionary of Plants, Their Classification and Uses* (Cambridge Univ. Press, ed. 3, 2008).
55. R. J. Hijmans, S. E. Cameron, J. L. Parra, P. G. Jones, A. Jarvis, Very high resolution interpolated climate surfaces for global land areas. *Int. J. Climatol.* **25**, 1965–1978 (2005). [doi:10.1002/joc.1276](https://doi.org/10.1002/joc.1276)
56. M. New, D. Lister, M. Hulme, I. Makin, A high-resolution data set of surface climate over global land areas. *Clim. Res.* **21**, 1–25 (2002). [doi:10.3354/cr021001](https://doi.org/10.3354/cr021001)
57. C. Körner, *Alpine Plant Life: Functional Plant Ecology of High Mountain Ecosystems* (Springer, 1999).
58. P. G. Allen, L. S. Pereira, D. Raes, M. Smith, “Crop evapotranspiration: Guidelines for computing crop requirements. Irrigation and Drainage Paper No. 56” (Food and Agriculture Organisation, 1998).
59. T. W. Davis, I. C. Prentice, B. D. Stocker, R. T. Thomas, R. J. Whitley, H. Wang, B. J. Evans, A. V. Gallego-Sala, M. T. Sykes, W. Cramer, Simple process-led algorithms for simulating habitats (SPLASH v.1.0): Robust indices of radiation, evapotranspiration and plant-available moisture. *Geosci. Model Dev.* **10**, 689–708 (2017). [doi:10.5194/gmd-10-689-2017](https://doi.org/10.5194/gmd-10-689-2017)
60. E. T. Linacre, Estimating the net-radiation flux. *Agric. Meteorol.* **5**, 49–63 (1968). [doi:10.1016/0002-1571\(68\)90022-8](https://doi.org/10.1016/0002-1571(68)90022-8)
61. K. Kikuzawa, Y. Onoda, I. J. Wright, P. B. Reich, Mechanisms underlying global temperature-related patterns in leaf longevity. *Glob. Ecol. Biogeogr.* **22**, 982–993 (2013). [doi:10.1111/geb.12042](https://doi.org/10.1111/geb.12042)

62. A. J. Kerkhoff, B. J. Enquist, Multiplicative by nature: Why logarithmic transformation is necessary in allometry. *J. Theor. Biol.* **257**, 519–521 (2009). [doi:10.1016/j.jtbi.2008.12.026](https://doi.org/10.1016/j.jtbi.2008.12.026)
63. A. T. Moles, D. I. Warton, L. Warman, N. G. Swenson, S. W. Laffan, A. E. Zanne, A. Pitman, F. A. Hemmings, M. R. Leishman, Global patterns in plant height. *J. Ecol.* **97**, 923–932 (2009). [doi:10.1111/j.1365-2745.2009.01526.x](https://doi.org/10.1111/j.1365-2745.2009.01526.x)
64. G. S. Campbell, J. M. Norman, in *Plant Canopies: Their Growth, Form and Function*, G. Russell, B. Marshall, P. G. Jarvis, Eds. (Cambridge Univ. Press, 1989), pp. 1–19.
65. T. J. Givnish, in *Theoretical Plant Morphology*, R. Sattler, Ed. (Leiden Univ. Press, 1978), pp. 83–142.
66. C. H. B. Priestley, R. J. Taylor, On the assessment of surface heat flux and evaporation using large-scale parameters. *Mon. Weather Rev.* **100**, 81–92 (1972). [doi:10.1175/1520-0493\(1972\)100<0081:OTAOSH>2.3.CO;2](https://doi.org/10.1175/1520-0493(1972)100<0081:OTAOSH>2.3.CO;2)
67. W. Cramer, I. C. Prentice, Simulation of regional soil moisture deficits on a European scale. *Nor. Geogr. Tidsskr.* **42**, 149–151 (1988). [doi:10.1080/00291958808552193](https://doi.org/10.1080/00291958808552193)
68. I. Harris, P. D. Jones, T. J. Osborn, D. H. Lister, Updated high-resolution grids of monthly climatic observations—The CRU TS3.10 Dataset. *Int. J. Climatol.* **34**, 623–642 (2014). [doi:10.1002/joc.3711](https://doi.org/10.1002/joc.3711)
69. M. D. Abrams, S. A. Mostoller, Gas exchange, leaf structure and nitrogen in contrasting successional tree species growing in open and understory sites during a drought. *Tree Physiol.* **15**, 361–370 (1995). [doi:10.1093/treephys/15.6.361](https://doi.org/10.1093/treephys/15.6.361) [Medline](#)
70. M. Aiba, T. Nakashizuka, Sapling structure and regeneration strategy in 18 *Shorea* species co-occurring in a tropical rainforest. *Ann. Bot.* **96**, 313–321 (2005). [doi:10.1093/aob/mci179](https://doi.org/10.1093/aob/mci179) [Medline](#)
71. Y. Basset, R. Hoft, Can apparent leaf damage in tropical trees be predicted by herbivore load or host-related variables? A case study in Papua New Guinea. *Selbyana* **15**, 3–13 (1994).
72. M. R. T. Boeger, C. Wisniewski, Comparação da morfologia foliar de espécies arbóreas de três estádios sucessionais distintos de floresta ombrófila densa (Floresta Atlântica) no Sul do Brasil. *Rev. Bras. Bot. Braz. J. Bot.* **26**, 61–72 (2003). [doi:10.1590/S0100-84042003000100007](https://doi.org/10.1590/S0100-84042003000100007)
73. M. R. T. Boeger, L. C. Alves, R. R. B. Negrelle, Leaf morphology of 89 tree species from a lowland tropical rain forest (Atlantic Forest) in South Brazil. *Braz. Arch. Biol. Technol.* **47**, 933–943 (2004). [doi:10.1590/S1516-89132004000600013](https://doi.org/10.1590/S1516-89132004000600013)
74. G. E. Burrows, Comparative anatomy of the photosynthetic organs of 39 xeromorphic species from subhumid New South Wales, Australia. *Int. J. Plant Sci.* **162**, 411–430 (2001). [doi:10.1086/319579](https://doi.org/10.1086/319579)
75. A. M. Camerik, M. J. A. Werger, Leaf characteristics of the flora of the high plateau of Itatiaia Brazil. *Biotropica* **13**, 39–48 (1981). [doi:10.2307/2387869](https://doi.org/10.2307/2387869)

76. J. D. Chinea, R. J. Beymer, C. Rivera, I. Sastre de Jesus, F. N. Scatena, "An annotated list of the flora of the Bisley Area, Luquillo Experimental Forest, Puerto Rico 1987 to 1992," U.S. Department of Agriculture, General Technical Report (1993), vol. SO-94, pp. 1–12.
77. J. Comstock, J. Ehleringer, Effect of variations in leaf size on morphology and photosynthetic rate of twigs. *Funct. Ecol.* **4**, 209–222 (1990). [doi:10.2307/2389340](https://doi.org/10.2307/2389340)
78. W. K. Cornwell, D. D. Ackerly, Community assembly and shifts in plant trait distributions across an environmental gradient in coastal California. *Ecol. Monogr.* **79**, 109–126 (2009). [doi:10.1890/07-1134.1](https://doi.org/10.1890/07-1134.1)
79. T. B. Croat, *Flora of Barro Colorado Island* (Stanford Univ. Press, 1978).
80. S. A. Cunningham, B. Summerhayes, M. Westoby, Evolutionary divergences in leaf structure and chemistry, comparing rainfall and soil nutrient gradients. *Ecol. Monogr.* **69**, 569–588 (1999). [doi:10.1890/0012-9615\(1999\)069\[0569:EDILSA\]2.0.CO;2](https://doi.org/10.1890/0012-9615(1999)069[0569:EDILSA]2.0.CO;2)
81. S. Díaz, J. G. Hodgson, K. Thompson, M. Cabido, J. H. C. Cornelissen, A. Jalili, G. Montserrat-Martí, J. P. Grime, F. Zarrinkamar, Y. Asri, S. R. Band, S. Basconcelo, P. Castro-Díez, G. Funes, B. Hamzehee, M. Khoshnevi, N. Pérez-Harguindeguy, M. C. Pérez-Rontomé, F. A. Shirvany, F. Vendramini, S. Yazdani, R. Abbas-Azimi, A. Bogaard, S. Boustani, M. Charles, M. Dehghan, L. de Torres-Espuny, V. Falczuk, J. Guerrero-Campo, A. Hynd, G. Jones, E. Kowsary, F. Kazemi-Saeed, M. Maestro-Martínez, A. Romo-Díez, S. Shaw, B. Siavash, P. Villar-Salvador, M. R. Zak, The plant traits that drive ecosystems: Evidence from three continents. *J. Veg. Sci.* **15**, 295–304 (2004). [doi:10.1111/j.1654-1103.2004.tb02266.x](https://doi.org/10.1111/j.1654-1103.2004.tb02266.x)
82. E. J. Edwards, Correlated evolution of stem and leaf hydraulic traits in *Pereskia* (Cactaceae). *New Phytol.* **172**, 479–789 (2006). [doi:10.1111/j.1469-8137.2006.01850.x](https://doi.org/10.1111/j.1469-8137.2006.01850.x) [Medline](#)
83. D. S. Falster, M. Westoby, Alternative height strategies among 45 dicot rain forest species from tropical Queensland, Australia. *J. Ecol.* **93**, 521–535 (2005). [doi:10.1111/j.0022-0477.2005.00992.x](https://doi.org/10.1111/j.0022-0477.2005.00992.x)
84. N. Fetcher, Leaf size and leaf temperature in tropical vines. *Am. Nat.* **117**, 1011–1014 (1981). [doi:10.1086/283787](https://doi.org/10.1086/283787)
85. L. M. Fliervoet, J. P. M. Van De Ven, Leaf characteristics of grassland in a microgradient of temperature and moisture conditions. *Phytocoenologia* **12**, 479–493 (1984). [doi:10.1127/phyto/12/1984/479](https://doi.org/10.1127/phyto/12/1984/479)
86. P. G. McDonald, C. R. Fonseca, J. M. Overton, M. Westoby, Leaf-size divergence along rainfall and soil-nutrient gradients: Is the method of size reduction common among clades? *Funct. Ecol.* **17**, 50–57 (2003). [doi:10.1046/j.1365-2435.2003.00698.x](https://doi.org/10.1046/j.1365-2435.2003.00698.x)
87. H. K. Gamage, M. S. Ashton, B. M. R. Singhakumara, Leaf structure of *Syzygium* spp. (Myrtaceae) in relation to site affinity within a tropical rain forest. *Bot. J. Linn. Soc.* **141**, 365–377 (2003). [doi:10.1046/j.1095-8339.2003.00138.x](https://doi.org/10.1046/j.1095-8339.2003.00138.x)
88. G. Joel, G. Aplet, P. M. Vitousek, Leaf morphology along environmental gradients in Hawaiian *Metrosideros polymorpha*. *Biotropica* **26**, 17–22 (1994). [doi:10.2307/2389106](https://doi.org/10.2307/2389106)
89. J. Giliberto, H. Estay, Seasonal water stress in some Chilean matorral shrubs. *Bot. Gaz.* **139**, 236–240 (1978). [doi:10.1086/336995](https://doi.org/10.1086/336995)

90. E. M. Goble-Garratt, D. T. Bell, W. A. Loneragan, Floristic and leaf structure patterns along a shallow elevational gradient. *Aust. J. Bot.* **29**, 329–348 (1981). [doi:10.1071/BT9810329](https://doi.org/10.1071/BT9810329)
91. L. Gratani, A. Bombelli, Differences in leaf traits among Mediterranean broad-leaved evergreen shrubs. *Ann. Bot. Fenn.* **38**, 15–24 (2001).
92. P. J. Grubb, E. V. J. Tanner, Montane forests and soils of Jamaica—Reassessment. *J. Arnold Arbor.* **57**, 313–368 (1976).
93. P. J. Grubb, E. A. Grubb, I. Miyata, Leaf structure and function in evergreen trees and shrubs of Japanese warm temperate rain forest. I. Structure of the lamina. *Bot. Mag. Tokyo* **88**, 197–211 (1975). [doi:10.1007/BF02489306](https://doi.org/10.1007/BF02489306)
94. A. K. Hegazy, M. I. El Amry, Leaf temperature of desert sand dune plants: Perspectives on the adaptability of leaf morphology. *Afr. J. Ecol.* **36**, 34–43 (1998). [doi:10.1046/j.1365-2028.1998.109-89109.x](https://doi.org/10.1046/j.1365-2028.1998.109-89109.x)
95. D. Holscher, S. Schmitt, K. Kupfer, Growth and leaf traits of four broad-leaved tree species along a hillside gradient. *Forstwissenschaftliches Centralblatt* **121**, 229–239 (2002). [doi:10.1046/j.1439-0337.2002.02031.x](https://doi.org/10.1046/j.1439-0337.2002.02031.x)
96. D. Hölscher, C. Leuschner, K. Bohman, J. Juhrendt, S. Tjitrosemito, Photosynthetic characteristics in relation to leaf traits in eight co-existing pioneer tree species in Central Sulawesi, Indonesia. *J. Trop. Ecol.* **20**, 157–164 (2004). [doi:10.1017/S0266467403001251](https://doi.org/10.1017/S0266467403001251)
97. D. Hölscher, C. Leuschner, K. Bohman, M. Hagemeyer, J. Juhrendt, S. Tjitrosemito, Leaf gas exchange of trees in old-growth and young secondary forest stands in Sulawesi, Indonesia. *Trees (Berl.)* **20**, 278–285 (2006). [doi:10.1007/s00468-005-0040-4](https://doi.org/10.1007/s00468-005-0040-4)
98. M. Kappelle, M. E. Leal, Changes in leaf morphology and foliar nutrient status along a successional gradient in a Costa Rican upper montane *Quercus* forest. *Biotropica* **28**, 331–344 (1996). [doi:10.2307/2389197](https://doi.org/10.2307/2389197)
99. D. L. Kelly, E. V. J. Tanner, V. Kapos, T. A. Dickinson, G. A. Goodfriend, P. Fairbairn, Jamaican limestone forests: Floristics structure and environment of three examples along a rainfall gradient. *J. Trop. Ecol.* **4**, 121–156 (1988). [doi:10.1017/S0266467400002649](https://doi.org/10.1017/S0266467400002649)
100. I. Kim, Comparative anatomy of some parents and hybrids of the Hawaiian *Madiinae* (Asteraceae). *Am. J. Bot.* **74**, 1224–1238 (1987). [doi:10.2307/2444158](https://doi.org/10.2307/2444158)
101. D. A. King, Tree allometry, leaf size and adult tree size in old-growth forests of western Oregon. *Tree Physiol.* **9**, 369–381 (1991). [doi:10.1093/treephys/9.3.369](https://doi.org/10.1093/treephys/9.3.369) [Medline](#)
102. T. Kohyama, Significance of architecture and allometry in saplings. *Funct. Ecol.* **1**, 399–404 (1987). [doi:10.2307/2389797](https://doi.org/10.2307/2389797)
103. R. Kooyman, M. Rossetto, W. Cornwell, M. Westoby, Phylogenetic tests of community assembly across regional to continental scales in tropical and subtropical rain forests. *Glob. Ecol. Biogeogr.* **20**, 707–716 (2011). [doi:10.1111/j.1466-8238.2010.00641.x](https://doi.org/10.1111/j.1466-8238.2010.00641.x)
104. C. Körner, A. Allison, H. Hilscher, Altitudinal variation of leaf diffusive conductance and leaf anatomy in heliophytes of montane New Guinea and their interrelation with microclimate. *Flora* **174**, 91–135 (1983). [doi:10.1016/S0367-2530\(17\)31377-4](https://doi.org/10.1016/S0367-2530(17)31377-4)

105. G. Kudo, A review of ecological studies on leaf-trait variations along environmental gradients - In the case of tundra plants. *Jap. J. Ecol.* **49**, 21–35 (1999).
106. M. R. Leishman, M. Westoby, Classifying plants into groups on the basis of associations of individual traits evidence from Australian semiarid woodlands, classifying plants into groups on the basis of associations of individual traits—Evidence from Australian semi-arid woodlands. *J. Ecol.* **80**, 417–424 (1992). [doi:10.2307/2260687](https://doi.org/10.2307/2260687)
107. J. W. Leverenz, D. Whitehead, G. H. Stewart, Quantitative analyses of shade-shoot architecture of conifers native to New Zealand. *Trees (Berl.)* **15**, 42–49 (2000). [doi:10.1007/s004680000067](https://doi.org/10.1007/s004680000067)
108. J. P. Lewis, E. F. Pire, I. M. Barberis, Structure, physiognomy and floristic composition of a *Schinopsis balansae* (Anacardiaceae) forest in the southern Chaco, Argentina. *Rev. Biol. Trop.* **45**, 1013–1020 (1997).
109. Y. L. Li, D. A. Johnson, Y. Z. Su, J. Y. Cui, T. H. Zhang, Specific leaf area and leaf dry matter content of plants growing in sand dunes. *Bot. Bull. Acad. Sin.* **46**, 127–134 (2005).
110. S. McIntyre, T. G. Martin, K. M. Heard, J. Kinloch, Plant traits predict impact of invading species: An analysis of herbaceous vegetation in the subtropics. *Aust. J. Bot.* **53**, 757–770 (2005). [doi:10.1071/BT05088](https://doi.org/10.1071/BT05088)
111. E. Medina, M. Sobrado, R. Herrera, Significance of leaf orientation for leaf temperature in an Amazonian sclerophyll vegetation. *Radiat. Environ. Biophys.* **15**, 131–140 (1978). [doi:10.1007/BF01323262](https://doi.org/10.1007/BF01323262) [Medline](#)
112. A. T. Moles, B. Peco, I. R. Wallis, W. J. Foley, A. G. B. Poore, E. W. Seabloom, P. A. Vesk, A. J. Bisigato, L. Cella-Pizarro, C. J. Clark, P. S. Cohen, W. K. Cornwell, W. Edwards, R. Ejrnaes, T. Gonzales-Ojeda, B. J. Graae, G. Hay, F. C. Lumbwe, B. Magaña-Rodríguez, B. D. Moore, P. L. Peri, J. R. Poulsen, J. C. Stegen, R. Veldtman, H. von Zeipel, N. R. Andrew, S. L. Boulter, E. T. Borer, J. H. C. Cornelissen, A. G. Farji-Brener, J. L. DeGabriel, E. Jurado, L. A. Kyhn, B. Low, C. P. H. Mulder, K. Reardon-Smith, J. Rodríguez-Velázquez, A. De Fortier, Z. Zheng, P. G. Blendinger, B. J. Enquist, J. M. Facelli, T. Knight, J. D. Majer, M. Martínez-Ramos, P. McQuillan, F. K. C. Hui, Correlations between physical and chemical defences in plants: Tradeoffs, syndromes, or just many different ways to skin a herbivorous cat? *New Phytol.* **198**, 252–263 (2013). [doi:10.1111/nph.12116](https://doi.org/10.1111/nph.12116) [Medline](#)
113. F. Molina-Freaner, C. Tinoco-Ojanguren, Vines of a desert plant community in Central Sonora, Mexico. *Biotropica* **29**, 46–56 (1997). [doi:10.1111/j.1744-7429.1997.tb00005.x](https://doi.org/10.1111/j.1744-7429.1997.tb00005.x)
114. H. A. Mooney, P. J. Ferrar, R. O. Slatyer, Photosynthetic capacity and carbon allocation patterns in diverse growth forms of *Eucalyptus*. *Oecologia* **36**, 103–111 (1978). [doi:10.1007/BF00344575](https://doi.org/10.1007/BF00344575) [Medline](#)
115. T. Navarro, C. L. Alados, B. Cabezudo, Changes in plant functional types in response to goat and sheep grazing in two semi-arid shrublands of SE Spain. *J. Arid Environ.* **64**, 298–322 (2006). [doi:10.1016/j.jaridenv.2005.05.005](https://doi.org/10.1016/j.jaridenv.2005.05.005)
116. U. Niinemets, A. Portsmouth, M. Tobias, Leaf size modifies support biomass distribution among stems, petioles and mid-ribs in temperate plants. *New Phytol.* **171**, 91–104 (2006). [doi:10.1111/j.1469-8137.2006.01741.x](https://doi.org/10.1111/j.1469-8137.2006.01741.x) [Medline](#)

117. P. Parolin, Seasonal changes of specific leaf mass and leaf size in trees of Amazonian floodplains. *Phyton (Horn)* **42**, 169–185 (2002).
118. S. Patiño, N. M. Fyllas, T. R. Baker, R. Paiva, C. A. Quesada, A. J. B. Santos, M. Schwarz, H. ter Steege, O. L. Phillips, J. Lloyd, Coordination of physiological and structural traits in Amazon forest trees. *Biogeosciences* **9**, 775–801 (2012). [doi:10.5194/bg-9-775-2012](https://doi.org/10.5194/bg-9-775-2012)
119. P. J. Peeters, Correlations between leaf constituent levels and the densities of herbivorous insect guilds in an Australian forest. *Austral Ecol.* **27**, 658–671 (2002). [doi:10.1046/j.1442-9993.2002.01227.x](https://doi.org/10.1046/j.1442-9993.2002.01227.x)
120. M. Pyykkö, Morphology and anatomy of leaves from some woody plants in a humid tropical forest of Venezuelan Guayana. *Acta Bot. Fenn.* **112**, 1–41 (1979).
121. S. J. Richardson, D. A. Peltzer, R. B. Allen, M. S. McGlone, R. L. Parfitt, Rapid development of phosphorus limitation in temperate rainforest along the Franz Josef soil chronosequence. *Oecologia* **139**, 267–276 (2004). [doi:10.1007/s00442-004-1501-y](https://doi.org/10.1007/s00442-004-1501-y) [Medline](#)
122. B. Rollet, in *Stratification of Tropical Forests as Seen in Leaf Structure, Part 2*, B. Rollet, C. H. Hoegermann, I. Roth, Eds. (Kluwer Academic Publishers, 1990), vol. 21.
123. I. Roth, Leaf structure: Coastal vegetation and mangroves of Venezuela, in *Handbuch der Pflanzenanatomie/Encyclopedia of Plant Anatomy*, vol. XIV, part 2 (1992).
124. I. Roth, T. M. de Bifano, Morphological and anatomical studies of leaves of the plants of a Venezuelan cloud forest. Part 1. Shape and size of the leaves. *Acta Biol. Venez.* **7**, 127–155 (1971).
125. D. L. Royer, P. Wilf, D. A. Janesko, E. A. Kowalski, D. L. Dilcher, Correlations of climate and plant ecology to leaf size and shape: Potential proxies for the fossil record. *Am. J. Bot.* **92**, 1141–1151 (2005). [doi:10.3732/ajb.92.7.1141](https://doi.org/10.3732/ajb.92.7.1141) [Medline](#)
126. G. J. Seiler, L. G. Campbell, Effect of Calculation technique on the estimation of leaf area in a mixed deciduous forest and oak-savanna woodland of southeastern North Dakota USA. *Prairie Nat.* **19**, 239–250 (1987).
127. G. R. Shaver, F. S. Chapin III, Production biomass relationships and element cycling in contrasting arctic vegetation types. *Ecol. Monogr.* **61**, 1–31 (1991). [doi:10.2307/1942997](https://doi.org/10.2307/1942997)
128. L. M. Shields, Leaf xeromorphy in dicotyledon species from a gypsum sand deposit. *Am. J. Bot.* **38**, 175–190 (1951). [doi:10.2307/2438067](https://doi.org/10.2307/2438067)
129. R. J. Scholes, P. G. H. Frost, Y. H. Tian, Canopy structure in savannas along a moisture gradient on Kalahari sands. *Glob. Change Biol.* **10**, 292–302 (2004). [doi:10.1046/j.1365-2486.2003.00703.x](https://doi.org/10.1046/j.1365-2486.2003.00703.x)
130. G. F. Midgley, SAFARI 2000 Leaf Measurements of Dominant Trees, Kalahari Sites, Wet Season 2000; data set available online at <http://daac.ornl.gov> or from Oak Ridge National Laboratory Distributed Active Archive Center, Oak Ridge, Tennessee, U.S.A., (2005).
131. M. D. Smith, A. K. Knapp, Physiological and morphological traits of exotic, invasive exotic, and native plant species in tallgrass prairie. *Int. J. Plant Sci.* **162**, 785–792 (2001). [doi:10.1086/320774](https://doi.org/10.1086/320774)

132. D. C. Steart, D. R. Greenwood, P. I. Boon, Paleocological implications of differential biomass and litter production in canopy trees in Australian *Nothofagus* and *Eucalyptus* forests. *Palaios* **20**, 452–462 (2005). [doi:10.2110/palo.2004.P04-57](https://doi.org/10.2110/palo.2004.P04-57)
133. F. J. Sterck, Crown development in tropical rain forest trees in gaps and understorey. *Plant Ecol.* **143**, 89–98 (1999). [doi:10.1023/A:1009889414418](https://doi.org/10.1023/A:1009889414418)
134. A. M. Sugden, Leaf anatomy in a Venezuelan montane forest. *Bot. J. Linn. Soc.* **90**, 231–241 (1985). [doi:10.1111/j.1095-8339.1985.tb00383.x](https://doi.org/10.1111/j.1095-8339.1985.tb00383.x)
135. S. Sun, D. Jin, P. Shi, The leaf size-twig size spectrum of temperate woody species along an altitudinal gradient: An invariant allometric scaling relationship. *Ann. Bot.* **97**, 97–107 (2006). [doi:10.1093/aob/mcj004](https://doi.org/10.1093/aob/mcj004) [Medline](#)
136. S. Sun, D. Jin, R. Li, Leaf emergence in relation to leaf traits in temperate woody species in East-Chinese *Quercus fabri* forests. *Acta Oecol.* **30**, 212–222 (2006). [doi:10.1016/j.actao.2006.04.001](https://doi.org/10.1016/j.actao.2006.04.001)
137. C. Q. Tang, M. Ohsawa, Zonal transition of evergreen, deciduous, and coniferous forests along the altitudinal gradient on a humid subtropical mountain, Mt. Emei, Sichuan, China. *Plant Ecol.* **133**, 63–78 (1997). [doi:10.1023/A:1009729027521](https://doi.org/10.1023/A:1009729027521)
138. C. Q. Tang, M. Ohsawa, Altitudinal distribution of evergreen broad-leaved trees and their leaf-size pattern on a humid subtropical mountain, Mt. Emei, Sichuan, China. *Plant Ecol.* **145**, 221–233 (1999). [doi:10.1023/A:1009856020744](https://doi.org/10.1023/A:1009856020744)
139. I. M. Turner, B. L. Ong, H. T. W. Tan, Vegetation analysis, leaf structure and nutrient status of a Malaysian heath community. *Biotropica* **27**, 2–12 (1995). [doi:10.2307/2388897](https://doi.org/10.2307/2388897)
140. N. Velázquez-Rosas, J. Meave, S. Vazquez-Santana, Elevational variation of leaf traits in montane rain forest tree species at La Chinantla, Southern Mexico. *Biotropica* **34**, 534–546 (2002). [doi:10.1646/0006-3606\(2002\)034\[0534:EVOLTI\]2.0.CO;2](https://doi.org/10.1646/0006-3606(2002)034[0534:EVOLTI]2.0.CO;2)
141. P. S. White, Corner's Rules in eastern deciduous trees: Allometry and its implications for the adaptive architecture of trees. *Bull. Torrey Bot. Club* **110**, 203–212 (1983). [doi:10.2307/2996342](https://doi.org/10.2307/2996342)
142. A. P. Withrow, Life forms and leaf size classes of certain plant communities of the Cincinnati region. *Ecology* **13**, 12–35 (1932). [doi:10.2307/1932488](https://doi.org/10.2307/1932488)
143. J. G. Bragg, M. Westoby, Leaf size and foraging for light in a sclerophyll woodland. *Funct. Ecol.* **16**, 633–639 (2002). [doi:10.1046/j.1365-2435.2002.00661.x](https://doi.org/10.1046/j.1365-2435.2002.00661.x)
144. D. S. Falster, M. Westoby, Leaf size and angle vary widely across species: What consequences for light interception? *New Phytol.* **158**, 509–525 (2003). [doi:10.1046/j.1469-8137.2003.00765.x](https://doi.org/10.1046/j.1469-8137.2003.00765.x)
145. K. P. Hogan, A. P. Smith, M. Samaniego, Gas exchange in six tropical semi-deciduous forest canopy tree species during the wet and dry seasons. *Biotropica* **27**, 324–333 (1995). [doi:10.2307/2388918](https://doi.org/10.2307/2388918)
146. H. Zhu, Ecological and biogeographical studies on the tropical rain forest of south Yunnan, SW China with a special reference to its relation with rain forests of tropical Asia. *J. Biogeogr.* **24**, 647–662 (1997). [doi:10.1111/j.1365-2699.1997.tb00075.x](https://doi.org/10.1111/j.1365-2699.1997.tb00075.x)

147. I. J. Wright, M. Westoby, Leaves at low versus high rainfall: Coordination of structure, lifespan and physiology. *New Phytol.* **155**, 403–416 (2002). [doi:10.1046/j.1469-8137.2002.00479.x](https://doi.org/10.1046/j.1469-8137.2002.00479.x)
148. M. Westoby, I. J. Wright, The leaf size-twig size spectrum and its relationship to other important spectra of variation among species. *Oecologia* **135**, 621–628 (2003). [doi:10.1007/s00442-003-1231-6](https://doi.org/10.1007/s00442-003-1231-6) [Medline](#)
149. C. Read, I. J. Wright, M. Westoby, Scaling up from leaf to canopy-aggregate properties in sclerophyll shrub species. *Austral Ecol.* **31**, 310–316 (2006). [doi:10.1111/j.1442-9993.2006.01559.x](https://doi.org/10.1111/j.1442-9993.2006.01559.x)
150. E. L. J. Little, F. H. Wadsworth, “Common trees of Puerto Rico and the Virgin Islands. US Department of Agriculture, Agriculture Handbook 249, in *U.S. Department of Agriculture, Agriculture Handbook 249* (U.S. Department of Agriculture, 1964).
151. E. L. J. Little, R. O. Woodbury, F. H. Wadsworth, U.S. Department of Agriculture, “Trees of Puerto Rico and the Virgin Islands, Volume 2, U.S. Department of Agriculture, Agriculture Handbook 449, in *U.S. Department of Agriculture, Agriculture Handbook 449* (1974), pp. 1024.
152. P. Acevedo-Rodriguez, R. O. Woodbury, in *Los Bejucos de Puerto Rico, Volumen 1*. (U.S. Department of Agriculture, 1985), vol. SO-58, pp. 1–331.
153. R. Villar, J. Merino, Comparison of leaf construction costs in woody species with differing leaf life-spans in contrasting ecosystems. *New Phytol.* **151**, 213–226 (2001). [doi:10.1046/j.1469-8137.2001.00147.x](https://doi.org/10.1046/j.1469-8137.2001.00147.x)
154. J. H. C. Cornelissen, A triangular relationship between leaf size and seed size among woody species: Allometry, ontogeny, ecology and taxonomy. *Oecologia* **118**, 248–255 (1999). [doi:10.1007/s004420050725](https://doi.org/10.1007/s004420050725) [Medline](#)
155. E. Garnier, P. Cordonnier, J.-L. Guillermin, L. Sonié, Specific leaf area and leaf nitrogen concentration in annual and perennial grass species growing in Mediterranean old-fields. *Oecologia* **111**, 490–498 (1997). [doi:10.1007/s004420050262](https://doi.org/10.1007/s004420050262) [Medline](#)
156. B. B. Lamont, P. K. Groom, R. M. Cowling, High leaf mass per area of related species assemblages may reflect low rainfall and carbon isotope discrimination rather than low phosphorus and nitrogen concentrations. *Funct. Ecol.* **16**, 403–412 (2002). [doi:10.1046/j.1365-2435.2002.00631.x](https://doi.org/10.1046/j.1365-2435.2002.00631.x)
157. D. D. Ackerly, P. B. Reich, Convergence and correlations among leaf size and function in seed plants: A comparative test using independent contrasts. *Am. J. Bot.* **86**, 1272–1281 (1999). [doi:10.2307/2656775](https://doi.org/10.2307/2656775) [Medline](#)
158. C. B. Lal, C. Annapurna, A. S. Raghubanshi, J. S. Singh, Foliar demand and resource economy of nutrients in dry tropical forest species. *J. Veg. Sci.* **12**, 5–14 (2001). [doi:10.1111/j.1654-1103.2001.tb02612.x](https://doi.org/10.1111/j.1654-1103.2001.tb02612.x)
159. S. Miyazawa, S. Satomi, I. Terashima, Slow leaf development of evergreen broad-leaved tree species in Japanese warm temperate forests. *Ann. Bot. (Lond.)* **82**, 859–869 (1998). [doi:10.1006/anbo.1998.0770](https://doi.org/10.1006/anbo.1998.0770)

160. H. Poorter, R. De Jong, A comparison of specific leaf area, chemical composition and leaf construction costs of field plants from 15 habitats differing in productivity. *New Phytol.* **143**, 163–176 (1999). [doi:10.1046/j.1469-8137.1999.00428.x](https://doi.org/10.1046/j.1469-8137.1999.00428.x)
161. F. Bongers, J. Popma, Leaf characteristics of the tropical rain forest flora of Los Tuxtlas, Mexico. *Bot. Gaz.* **151**, 354–365 (1990). [doi:10.1086/337836](https://doi.org/10.1086/337836)
162. J. Cavender-Bares, K. Kitajima, F. A. Bazzaz, Multiple trait associations in relation to habitat differentiation among 17 Floridian oak species. *Ecol. Monogr.* **74**, 635–662 (2004). [doi:10.1890/03-4007](https://doi.org/10.1890/03-4007)
163. N. S. Christodoulakis, K. A. Mitrakos, in *Plant Response to Stress*, J. D. Tenhunen, F. M. Catarino, O. L. Lange, W. C. Oechel, Eds. (Springer-Verlag, Berlin Heidelberg, 1987), pp. 547–551.
164. G. L. S. Chua *et al.*, The nutrient status of the plateau heath forest on Gunung Keriong, Pahang, Peninsular Malaysia. *J. Trop. For. Sci.* **8**, 240–246 (1995).
165. G. Kudo, U. Molau, N. Wada, Leaf-trait variation of tundra plants along a climatic gradient: An integration of responses in evergreen and deciduous species. *Arct. Antarct. Alp. Res.* **33**, 181–190 (2001). [doi:10.2307/1552219](https://doi.org/10.2307/1552219)
166. J. J. Midgley, G. R. Van Wyk, D. A. Everard, Leaf attributes of South African forest species. *Afr. J. Ecol.* **33**, 160–168 (1995). [doi:10.1111/j.1365-2028.1995.tb00791.x](https://doi.org/10.1111/j.1365-2028.1995.tb00791.x)
167. U. Niinemets, K. Kull, Leaf weight per area and leaf size of 85 Estonian woody species in relation to shade tolerance and light availability. *For. Ecol. Manage.* **70**, 1–10 (1994). [doi:10.1016/0378-1127\(94\)90070-1](https://doi.org/10.1016/0378-1127(94)90070-1)
168. I. Nitta, M. Ohsawa, Leaf dynamics and shoot phenology of eleven warm-temperature evergreen broad-leaved trees near their northern limit in central Japan. *Plant Ecol.* **130**, 71–88 (1997). [doi:10.1023/A:1009735709258](https://doi.org/10.1023/A:1009735709258)
169. N. Osada, H. Takeda, A. Furukawa, M. Awang, Leaf dynamics and maintenance of tree crowns in a Malaysian rain forest stand. *J. Ecol.* **89**, 774–782 (2001). [doi:10.1046/j.0022-0477.2001.00590.x](https://doi.org/10.1046/j.0022-0477.2001.00590.x)
170. L. D. Prior, D. Eamus, D. M. J. S. Bowman, Leaf attributes in the seasonally dry tropics: A comparison of four habitats in northern Australia. *Funct. Ecol.* **17**, 504–515 (2003). [doi:10.1046/j.1365-2435.2003.00761.x](https://doi.org/10.1046/j.1365-2435.2003.00761.x)
171. V. I. P'yankov, L. A. Ivanov, H. Lambers, Plant construction cost in the boreal species differing in their ecological strategies. *Russ. J. Plant Physiol.* **48**, 67–73 (2001). [doi:10.1023/A:1009002715572](https://doi.org/10.1023/A:1009002715572)
172. V. I. Pyankov, L. A. Ivanov, H. Lambers, Chemical composition of the leaves of plants with different ecological strategies from the boreal zone. *Russ. J. Ecol.* **32**, 221–229 (2001). [doi:10.1023/A:1011354019319](https://doi.org/10.1023/A:1011354019319)
173. B. Shipley, Structured interspecific determinants of specific leaf area in 34 species of herbaceous angiosperms. *Funct. Ecol.* **9**, 312–319 (1995). [doi:10.2307/2390579](https://doi.org/10.2307/2390579)

174. M. A. Sobrado, E. Medina, General morphology, anatomical structure, and nutrient content of sclerophyllous leaves of the 'bana' vegetation of amazonas. *Oecologia* **45**, 341–345 (1980). [doi:10.1007/BF00540202](https://doi.org/10.1007/BF00540202) [Medline](#)
175. I. M. Turner, H. T. W. Tan, Habitat-related variation in tree leaf form in four tropical forest types in Pulau Ubin, Singapore. *J. Veg. Sci.* **2**, 691–698 (1991). [doi:10.2307/3236179](https://doi.org/10.2307/3236179)
176. G. Williams-Linera, Leaf demography and leaf traits of temperate-deciduous and tropical evergreen-broadleaved trees in a Mexican montane cloud forest. *Plant Ecol.* **149**, 233–244 (2000). [doi:10.1023/A:1026508610236](https://doi.org/10.1023/A:1026508610236)
177. G. Zotz, M. T. Tyree, S. Patino, M. R. Carlton, Hydraulic architecture and water use of selected species from a lower montane forest in Panama. *Trees (Berl.)* **12**, 302–309 (1998). [doi:10.1007/s004680050155](https://doi.org/10.1007/s004680050155)
178. L. Poorter, F. Bongers, Leaf traits are good predictors of plant performance across 53 rain forest species. *Ecology* **87**, 1733–1743 (2006). [doi:10.1890/0012-9658\(2006\)87\[1733:LTAGPO\]2.0.CO;2](https://doi.org/10.1890/0012-9658(2006)87[1733:LTAGPO]2.0.CO;2) [Medline](#)
179. E. T. Linacre, Further notes on a feature of leaf and air temperatures. *Archmeteor. Geophys. Bioklimatol. Ser B Allg. Biol. Klimatol.* **15**, 422–436 (1967). [doi:10.1007/BF02390453](https://doi.org/10.1007/BF02390453)
180. R. Leuning, K. W. Cremer, Leaf temperatures during radiation frost Part I. Observations. *Agric. Meteorol.* **42**, 121–133 (1988). [doi:10.1016/0168-1923\(88\)90072-X](https://doi.org/10.1016/0168-1923(88)90072-X)
181. D. N. Jordan, W. K. Smith, Radiation frost susceptibility and the association between sky exposure and leaf size. *Oecologia* **103**, 43–48 (1995). [doi:10.1007/BF00328423](https://doi.org/10.1007/BF00328423) [Medline](#)